Pantophysin Is a Ubiquitously Expressed Synaptophysin Homologue and Defines Constitutive Transport Vesicles

Nikolas K. Haass, Jürgen Kartenbeck, and Rudolf E. Leube

Division of Cell Biology, German Cancer Research Center, D-69120 Heidelberg, Federal Republic of Germany

Abstract. Certain properties of the highly specialized synaptic transmitter vesicles are shared by constitutively occurring vesicles. We and others have thus identified a cDNA in various nonneuroendocrine cell types of rat and human that is related to synaptophysin, one of the major synaptic vesicle membrane proteins, which we termed pantophysin. Here we characterize the gene structure, mRNA and protein expression, and intracellular distribution of pantophysin. Its mRNA is detected in murine cell types of nonneuroendocrine as well as of neuroendocrine origin. The intron/exon structure of the murine pantophysin gene is identical to that of synaptophysin except for the last intron that is absent in pantophysin. The encoded polypeptide of calculated mol wt 28,926 shares many sequence features with synaptophysin, most notably the four hydrophobic putative transmembrane domains, although the cytoplasmic end domains are completely different. Using antibodies against the unique carboxy terminus pantophysin can be detected by immunofluorescence microscopy in both exocrine and endocrine cells of human pancreas, and in cultured cells, colocalizing with constitutive secretory and endocytotic vesicle markers in nonneuroendocrine cells and with synaptophysin in cDNA-transfected epithelial cells. By immunoelectron microscopy, the majority of pantophysin reactivity is detected at vesicles with a diameter of <100 nm that have a smooth surface and an electron-translucent interior. Using cell fractionation in combination with immunoisolation, these vesicles are enriched in a light fraction and shown to contain the cellular vSNARE cellubrevin and the ubiquitous SCAMPs in epithelial cells and synaptophysin in neuroendocrine or cDNA-transfected nonneuroendocrine cells and neuroendocrine tissues. Pantophysin is therefore a broadly distributed marker of small cytoplasmic transport vesicles independent of their content.

TRANSPORT between discontinuous cellular membranes is dependent on the presence of small carrier vesicles. Such vesicles have been identified and characterized in various pathways connecting, e.g., ER and Golgi apparatus, *cis*- and *trans*-Golgi cisternae, Golgi apparatus and lysosomes, *trans*-Golgi network and plasma membrane, or plasma membrane and endosomes (for description of such transport vesicles see references 4, 14, 28, 48, 51–53; for review see references 19, 56, 57). While it has been shown in many instances that the assembly of a defined "coat" is of importance for selective vesicle formation from a donor membrane (for example see references 2, 51, 55, 61, 65, 74), and that a multimolecular fusion complex is involved in vesicle fusion with a particular target membrane (for recent review see references 6, 20, 61, 66), very little is known about basic requirements for vesicle maintenance in the "free" cytoplasmic state.

A suitable model system to examine principles determining vesicle morphogenesis is the synaptic, transmitter-containing, small secretory vesicle in neurons. Its major components have been characterized, and were shown to be, in large part, highly specific (6, 66). Interestingly, basic molecular principles needed for structural and functional aspects of synaptic vesicle recycling are also shared by constitutive transport vesicles, and are conserved from yeast to human (5, 20).

Our interest has centered on synaptophysin (SPH)[1], one of the major integral membrane proteins of these transmitter-containing vesicles in neurons and of similar vesicles in cells of the dispersed neuroendocrine system (33, 42, 50, 67, 75, 76). The observation that synaptophysin is able to induce the formation of voltage-sensitive channels upon reconstitution into planar lipid bilayers (68), that synaptophysin binds to the vesicular SNAP receptor (v SNARE) synaptobrevin, preferably synaptobrevin-2, when it is not

Please address all correspondence to R.E. Leube, Division of Cell Biology, German Cancer Research Center, Im Neuenheimer Feld 280, D-69120 Heidelberg, Federal Republic of Germany. Tel.: 49 6221 423503. Fax: 49 6221 423404.

R.E. Leube's present address is Department of Anatomy, Johannes Gutenberg-University Maine, Becherweg 13, D-55099 Mainz, Federal Republic of Germany. Tel.: 49 6131 392731. Fax: 49 6131 393719.

1. *Abbreviations used in this paper*: KLH, keyhole limpet hemocyanine; LAMP, lysosomal membrane protein; PPH, pantophysin; SCAMP, secretory carrier-associated membrane protein; v SNARE, vesicular soluble N-ethylmaleimide sensitive factor attachment protein receptor, i.e., vesicular SNAP receptor; SPH, synaptophysin; TFR, transferrin receptor.

present in the docking complex (11, 16, 72), and that synaptophysin forms a freeze-thaw-sensitive complex together with synaptobrevin and subunits of the vacuolar ATPase (25, 62) all suggested that it is important for synaptic vesicle to function. However, ablation of the synaptophysin gene in mice did not affect growth, reproduction, or any other vital function under laboratory conditions, and functional synaptic vesicles were still present in these animals (17). It is therefore of interest to note that synaptophysin is a member of a growing multigene family that includes synaptoporin/synaptophysin II (23, 37), which is also a neuron-specific synaptic vesicle protein, and pantophysin (PPH) whose mRNA was recently identified on the basis of its similarity to that of synaptophysin (40; see also reference 77).

We now show that the pantophysin gene is closely related to that of synaptophysin, but that mRNA and protein are expressed ubiquitously in tissues and cultured cells where the great majority of pantophysin is localized in cytoplasmic microvesicles of various secretory, shuttling, and endocytotic recycling pathways. Pantophysin, together with other proteins with four membrane-spanning domains, may therefore fulfill basic housekeeping functions for all these small transport vesicles.

Materials and Methods

Reverse Transcription and Polymerase Chain Reaction

Reverse transcription of RNA with AMV reverse transcriptase and polymerase chain reaction using amplimers SY-O-92502 and SY-O-92501 to amplify synaptophysin-related genes (see 40) or CB-O-931608 (5′-AAA GGA TCC GCC GAA ATG TCT ACA GGG GTG-3′) and CB-O-931610 (5′-AAA AAG CTT CAT CTT GCA GTT CTT CCA CCA-3′) to amplify the cytoplasmic part of rat cellubrevin (47) were performed as described (40).

λ-Phage Isolation and Characterization

A gene bank in λ FIX II derived from genomic liver DNA of 129SVJ mice was purchased from Stratagene (La Jolla, CA). For isolation of pantophysin-encoding clones, a 536-bp BamHI–HindIII fragment was first amplified from 3T3-L1–derived cDNA with amplimers SY-92502 and SY-92501 (cf. 40), and cloned into pBluescriptII KS (+) (Stratagene) resulting in plasmid bPM1. The random prime-labeled BamHI–HindIII insert of bPM1 was then used for gene bank screening (2.2×10^6 phages) to isolate phage λPM1 that was shown by nucleotide sequencing to contain the entire 3′-part of the gene. For completion of the 5′-end, a 648-bp AccI–PstI fragment was taken from a subclone of the insert of λPM1 and used as a random prime-labeled probe in another round of library screening. Restriction maps were established for all isolated clones and overlapping fragments were subcloned into pBluescriptII KS (+) and subjected to nucleotide sequencing of both strands.

RNA Purification and Northern Blot Hybridization

RNA was purified from cultured cells following the procedure of Gough (27), and polyadenylated mRNA was further enriched by affinity chromatography using oligo(dT)-cellulose (Pharmacia, Uppsala, Sweden). Purified RNA was electrophoretically separated through formaldehyde-containing agarose gels and transferred onto Biodyne B nylon membranes (Pall, Portsmouth, UK) before hybridization with radioactively labeled riboprobes using standard procedures (cf. 40). For detection of murine pantophysin mRNA, plasmid cDNA clone bPM1 was linearized with HindIII, and labeled RNA was prepared with the help of T7-RNA-polymerase. After hybridization at 65°C under standard conditions (17), filters were washed briefly at room temperature and twice for 20 min at 68°C in 0.1 × SSC/0.1% SDS, treated with 50 μg/ml RNase A in 2 × SSC for 30 min at 37°C, washed three times for 10 min at room temperature, and 30 min at 68°C in 0.1 × SSC/0.1% SDS.

Cell Culture and Transfection

The following cell lines were used and propagated as described: Murine embryonic fibroblasts of line 3T3-L1 (ATCC CL 173), murine pituitary tumor cells of line AtT20 (ATCC CCL 89), murine pluripotent embryonic stem cells of line R1 (49), neuroendocrine rat adrenal pheochromocytoma cells of line PC12 (ATCC CRL 1721), epidermoid cells of human vulvar carcinoma line A431 (ATCC CRL 1555), hepatocellular carcinoma-derived PLC cells (ATCC CRL 8024), and stably synaptophysin-expressing sublines A431-5S4, established from A431 cells, and PLC-6S4, derived from PLC cells (44).

For transfection experiments several gene constructs were prepared. Oligonucleotides MY-O-941178 (5′-CGG AAC AAA AAC TGA TAT CCG AGG AAG ATC TGG-3′) and MY-O-941179 (5′-CGC CAG ATC TTC CTC GGA TAT CAG TTT TTG TTC-3′) coding for a defined myc epitope recognized by mAb MYC 1-9E10.2 (18) were inserted into the NarI site of human pantophysin-encoding clone pPH2 (40) to generate plasmid pMP1. For construction of pPM2, the myc epitope-coding sequence was inserted into the first intravesicular loop by cloning oligonucleotides MY-O-941180 (5′-GAA CAA AAA CTG ATA TCC GAG GAA GAT CTC CCT GCA-3′) and MY-O-941181 (5′-GGG AGA TCT TCC TCG GAT ATC AGT TTT TGT TCT GCA-3′) into the PstI site of pPH2. To add the cytoplasmic carboxy terminus of rat synaptophysin onto pantophysin, two fragments were amplified by PCR either from pPH2 (amplimers PH-O-931968 [5′-AAA AAG CTT ACG CAG TAT GGC GCC CAA CAT-3′] and PH-O-932292 [5′-AAA AGA TCT TAT TCC GGT AGG AGG TGG AAT-3′]) or pSR[5] (amplimers SY-O-92553 [5′-AAA GAT CTG GCG CCC CGG AAA AGC AAC C-3′] and SY-O-603 [5′-GTG GAT CCC CCG GGC TGC AGG-3′]), and combined after digestion with HindIII–BglII and BglII–PstI, respectively, in the HindIII–PstI-cleaved pBluescriptII KS (+) vector resulting in plasmid pPS1. To add the myc epitope onto the carboxy terminus of human pantophysin, the BglII–XbaI synaptophysin-containing fragment of pPS1 was substituted by oligonucleotides MY-O-94687 (5′-GAT CTG AAC AAA AAC TGA TAT CCG AGG AAG ATC T-3′) and MY-O-94688 (5′-CTA GAG ATC TTC CTC GGA TAT CAG TTT TTG TTC A-3′) to produce plasmid pPM1. The correct cloning was confirmed in each case by nucleic acid sequencing. Inserts were then further subcloned into the eukaryotic expression vectors pRC/CMV (Invitrogen, San Diego, CA) by integration of the appropriate fragments into HindIII–XbaI, or pBEHpac18 (31) by insertion of the appropriate fragments into KpnI–XbaI. Synaptophysin gene construct pSR[10] has been described (44).

Cells were transfected with purified DNA of appropriate gene constructs using the calcium phosphate coprecipitation method and selected as previously described (44, 69).

Expression of Recombinant Proteins in Escherichia Coli

The cytoplasmic end domains of human pantophysin were combined with vimentin to produce fusion proteins in *E. coli.* The amino terminus of human pantophysin was amplified with amplimers PH-O-95252 (5′-AAA CCA TGG CGC CCA ACA TCT ACT T-3′) and PH-O-95253 (5′-AAA CCA TGG GCT CCT TGA GCG GGT TGA G-3′) from plasmid pPH2 (cf. 40). The resulting fragment was cut with NcoI and combined with the NcoI–HindIII insert of the human vimentin-encoding plasmid clone pDS5N/Hum-Vim-SD1 (30) in the *E. coli* expression vector pET-21d(+) (Novagen, Madison, WI) generating plasmid clone pETPV2. The carboxy terminus of human pantophysin was amplified from pPH2 with amplimers PH-O-95256 (5′-AAA TCT AGA TAC AAG GAG ACC AGC CTA CA-3′) and PH-O-95257 (5′-AAA TCT AGA TTA TAT TCC GGT AGG AGG T-3′), and cloned after digestion with XbaI into the *E. coli* expression-plasmid pET3ad.vimentin.GFP (kindly provided by Dr. M. Klymkowsky, University of Colorado at Boulder, Boulder, CO) that encodes a chimera of *Xenopus laevis* vimentin-1 and green fluorescent protein and was originally derived from pETadVimentin-1.stop (13). The new plasmid was termed pETVP1.

Clone pAX-GalS1 coding for a fusion protein of β-galactosidase and the cytoplasmic carboxy terminus of rat synaptophysin in pAX5[+] (Medac, Hamburg, FRG) has been described recently (44).

To produce the cytoplasmic carboxy terminus of murine synaptoporin, a 210-bp fragment was amplified from the recently isolated synaptoporin cDNA clone pPO2 (17) with amplimers SO-O-951964 (5′-AAA GGA TCC TCA AGG AGA CTG GCT GGC AT-3′) and SO-O-951965 (5′-AAA AAG CTT TTA TAT CTG ATT GTT AAA GG-3′). The resulting frag-

ment was cleaved with BamHI and HindIII to be inserted into the BglII–HindIII sites of the prokaryotic expression vector pQE-42 (Qiagen, Chatsworth, CA) thereby creating construct DHFR-HisPo4 that encodes a fusion protein of dihydrofolate reductase with a poly-histidine tag and the carboxy terminus of murine synaptoporin.

The cytoplasmic amino terminus of rat cellubrevin was prepared from rat liver cDNA using amplimers CB-O-931608 and CB-O-931610 (see above), and the BamHI–HindIII-cleaved products were cloned into the prokaryotic expression vector pQE-9 (Qiagen) resulting in clone HisRCB2.

Recombinant proteins were expressed and purified from bacteria using protocols provided by Medac, Novagen, and Qiagen or those previously described (cf. 29, 41, 44).

Production and Purification of Antibodies

The following antigens were used for immunizations of rabbit and/or chicken: (*a*) synthetic oligopeptides P-PHC1 (KETSLHSPSNTSAPHSQGGC), P-PHC2 (LHSPSNTSAPHSQGGC) and P-PHC3 (CKETSLHSPSNTSAPHSQGGIPPPTGI), all taken from the cytoplasmic carboxy terminus of human pantophysin (the underlined cysteines were added for coupling to keyhole limpet hemocyanine [KLH]); (*b*) synthetic oligopeptide P-PHN1 (APNIYLVRQRISRLGQRMSGFQINLC) corresponding to the cytoplasmic amino terminus of human pantophysin (the underlined cysteine was also included for coupling); and (*c*) the recombinant histidine-tagged amino terminus of rat cellubrevin enriched from bacteria that were transformed with plasmid HisRCB2 (see above). Purified fusion proteins, peptides, or peptides coupled to maleimide-activated KLH (Pierce, Rockford, IL) were injected repeatedly with or without adjuvans at 3-wk intervals. Chicken antibodies were enriched from eggs first by careful removal of egg white from egg yolk. After washing with water, the yolk membrane was punctured, and the effluent was homogenized in 20 ml TBS-buffer (10 mM Tris-HCl, pH 7.5, 140 mM NaCl) per egg yolk. After addition of 20 ml chloroform, mixing and incubation at 4°C for 24 h, the mixture was centrifuged (5,000 *g*, 15 min, 20°C). The upper phase was transferred to smaller centrifuge tubes that were stored for 10 min on ice and recentrifuged (27,500 *g*, 15 min, 4°C). Ammonium sulfate was slowly added to the supernatant (final concentration: 29.1 *g*/100 ml). After incubation at 4°C for 10 min, antibodies were concentrated by centrifugation (12,000 *g*, 10 min, 4°C), and the pelleted material was dissolved in PBS and dialyzed against PBS.

Enriched chicken antibodies or sera produced in rabbits were further purified by affinity chromatography. To this end recombinant protein was coupled through a spacer to *N*-hydroxysuccinimide esther-activated agarose beads (Affi-Gel 10 from BioRad, Hercules, CA). Binding was done in 0.1 M MOPS, pH 7.5 for 4 h at 4°C. After several washes with 0.5 M sodium phosphate buffer (pH 7.5), the matrix was washed with 1 M NaCl/0.05 M sodium phosphate buffer (pH 7.5), and remaining binding sites were subsequently saturated by incubation in 100 mM ethanolamine (pH 7.5) overnight at 4°C. Serum diluted 1:10 in 10 mM Tris-HCl (pH 7.5) was then loaded on the column preequilibrated in the same buffer followed by extensive washing with 10 mM Tris-Cl (pH 7.5) and several washes with 0.5 M NaCl/10 mM Tris-HCl (pH 7.5). Specifically bound antibodies were eluted either with 100 mM glycine (pH 2.5) and/or 100 mM triethylamine (pH 11.5), and directly diluted 1:2 in 1 M Tris-HCl (pH 8.0). Affinity-purified antibodies were used either directly after dialysis against PBS or after ammonium sulfate precipitation.

Immunofluorescence and Immunoelectron Microscopy

The following antibodies were used: murine mAbs against synaptophysin (SY38; 75), secretory carrier-associated membrane proteins (SCAMPs) (SG7C12; kindly provided by Dr. J.D. Castle; 7), human transferrin receptor (TFR) (B3/25; Boehringer, Mannheim, FRG; H68.4 kindly provided by Dr. I.S. Trowbridge; 73), a defined myc epitope (MYC 1-9E10.2; ATCC CRL 1729; 18), and the lysosomal membrane proteins, LAMP-1 (antibody H4A3) and LAMP-2 (antibody H4B4), from the Developmental Studies Hybridoma Bank (Iowa City, IA), as well as affinity-purified antibodies from rabbit against β-COP (kindly provided by Dr. T. Kreis; "anti-EAGE" in 15).

For immunofluorescence microscopy, 5 μm cryosections were treated with acetone (−20°C, 10 min), and cultured cells were either fixed with methanol (−20°C, 5 min) and acetone (−20°C, 10 s), or after a brief treatment with saponin (0.1–0.5% for 10–40 s) with 2% formaldehyde (room temperature, 30 min). Cells were further processed as described (44) for single and double immunofluorescence, and viewed with a conventional epifluorescence microscope (Axiophot, Carl Zeiss, Jena, FRG) or a confocal laser scan microscope (LSM 410, Carl Zeiss). Laser scan images of double immunofluorescence labelings were obtained by simultaneous scanning of the sections in the same focal plane (thickness ~0.8 μm) with a helium-neon laser at λ = 543 nm and an argon-ion laser at λ = 488 nm measuring emission at λ = 590–610 nm and at λ = 510–525 nm. Secondary antibodies coupled to Texas red, the cyanine Cy2, or fluorescein-isothiocyanate were purchased from Dianova (Hamburg, FRG) or Biotrend (Köln, FRG).

For immunoelectron microscopy cells were grown to near confluency on glass coverslips. Cells were permeabilized by a gentle treatment with 0.04% saponin in PBS/1 mM $MgCl_2$ for 30 s. Primary affinity-purified antibodies were diluted with PBS/1 mM $MgCl_2$, and cells were incubated for 20 min at room temperature. After several washings in PBS/1 mM $MgCl_2$, cells were fixed with freshly prepared 2% formaldehyde for 20 min. After quenching with 50 mM NH_4Cl_2 in PBS for 2 × 5 min 6-nm-gold coupled secondary antibodies (Biotrend) were added at room temperature for up to 3 h. Several washings with PBS (2 × 3 min) followed and cells were postfixed and further processed for electron microscopy as described (44).

Cell Fractionation and Immunoblotting

Cultured cells and frozen tissue samples that were cut into small pieces were routinely lysed by suspension in H buffer (10 mM triethylamine-acetic acid, pH 7.4, 1 mM EGTA, 1 mM EDTA, 2 mM DTT, 2 μg/ml E-64, 40 μg/ml bestatin, 1 μg/ml pepstatin, and 20 μM APMSF) and homogenized with 30 up and down strokes in a tight-fitting Dounce homogenizer. In some experiments cell lysates were first centrifuged at 1,000 *g* for 10 min resulting in pellet P1 and supernatant S1 that was recentrifuged at 7,000 *g* for 10 min yielding pellet P2 and supernatant S2. Centrifugation of S2 at 15,000 *g* for 10 min generated pellet P3 and supernatant S3, and further centrifugation of S3 at 100,000 *g* for 30 min resulted in pellet P4 and supernatant S4. Extraction of either pellet fraction with Triton X-100 (incubation overnight in 1% Triton X-100 in H buffer) and recentrifugation at 100,000 *g* for 30 min produced pellet fractions P1′, P2′, P3′, and P4′ and the corresponding supernatants S1′, S2′, S3′, and S4′.

For immunoisolation 15,000 *g* supernatants were first prepared from homogenized cell or tissue lysates in H buffer. Magnetic beads (rat anti–mouse IgG1-coated Dynabeads M-450 and sheep anti–rabbit IgG-coated Dynabeads M-280) were obtained from Dynal (Hamburg, FRG). In addition, rabbit anti–chicken IgY antibodies (Sigma) were coupled to *p*-toluenesulfonylchloride–activated Dynabeads M-450 (Dynal) in the following way: 300 μg secondary antibody (in 2-ml coupling buffer containing 50 mM borate, pH 9.5) was added to 8×10^8 beads (~2 ml), and the mixture was incubated at room temperature for 24 h. After three washes for several hours with 10 × PBS/0.1% (wt/vol) BSA beads were resuspended in 10 × PBS/0.1% (wt/vol) BSA and stored at 4°C. 6.7×10^7 magnetic particles coated with appropriate secondary antibodies were incubated with primary antibodies for 2 h in 5 ml isolation buffer (10 mM EGTA, 250 mM sucrose, and 0.1% (wt/vol) BSA in PBS). Beads were washed three times for 10 min at room temperature in 5 ml isolation buffer, treated with blocking solution (10 mg/ml L-α-phosphatidylcholine (Sigma) isolation buffer) for 1 h, and incubated for 1 h with up to 10 mg protein obtained from 15,000 *g* supernatants. Subsequently, beads were first washed 5 × 10 min in isolation buffer, and then briefly in high salt buffer (1 M KCl in isolation buffer), and finally in isolation buffer (2 × 5 min). The immunoisolated material was either directly analyzed by SDS-PAGE and immunoblotting, or was fixed and embedded for electron microsocopy as described (44).

Linear sucrose gradients ranging from 15% (wt/vol) to 60% (wt/vol) sucrose for equilibrium gradient centrifugation or from 15% (wt/vol) to 45% (wt/vol) sucrose for velocity gradient centrifugation (the sucrose was dissolved in 10 mM triethylamine-acetic acid, pH 7.4, 1 mM EGTA, 1 mM EDTA, 2 mM DTT, and 2 μM APMSF) were layered on top of 70% (wt/vol) sucrose pads. Approximately 500–1,000 μg of protein contained in S1-fractions (50–200 μl) were loaded on top of each gradient, and centrifugation was performed in an SW40 Ti rotor (Beckman Instruments, Palo Alto, CA) at 8°C for either 17.5 h at 140,000 *g* (equilibrium gradients) or 160 min at 270,000 *g* (velocity gradients). Fractions were collected from top to bottom and further analyzed by an ELISA as recently described (39, 44).

Results

Similarities in Amino Acid Sequence and Gene Structure of Pantophysin and Synaptophysin

We recently identified, in reverse transcription-PCR ex-

periments, orthologous cDNAs in rat and human nonneuroendocrine cells that encode a protein which is related to the neuroendocrine vesicle protein synaptophysin, which we termed pantophysin (40). We have now used the same experimental approach to isolate and clone a murine pantophysin cDNA fragment from 3T3-L1 fibroblasts. The amplified cDNA in plasmid clone bPM1 showed significant homology to human and rat pantophysin (84.6% and 92.2% nucleic acid identity, respectively). To determine the gene structure of pantophysin, we used this cDNA to screen a murine λ-phage library. From the 21 clones isolated, the two phages λPM1 and λPM2 with overlapping inserts contained the entire pantophysin gene together with some additional flanking regions. The complete nucleic acid sequence was determined for the pantophysin gene of ~23 kb. Fig. 1 shows the entire derived amino acid sequence of the encoded polypeptide with a calculated mol wt of 28,926 including the start methionine. Murine pantophysin is 83% identical to the human orthologue (40) and shares a significant amino acid sequence identity with rat synaptophysin (43% identity; 42, 67). Pantophysin contains, similar to synaptophysin, four 23–29–amino acid long segments of significant hydrophobicity assumed to form transmembrane domains (see Fig. 1), which, in contrast to synaptophysin, are not predicted to be α helices (26). Other conserved features (Fig. 1) are a potential N-glycosylation site (for identification in rat synaptophysin see 43) in the first intravesicular loop domain (N_{72}), paired cysteine residues in both intravesicular loops (C_{64}, C_{99}, C_{194}, C_{202}), and charged residues within transmembrane domains (K_{37}, D_{154}) including the lysine residue in transmembrane segment 1 that was previously shown to be important for the correct topogenesis of synaptophysin (41). However, there are also properties that distinguish the pantophysins from the synaptophysins: they are highly basic (calculated isoelectric point 9.00 for murine pantophysin vs 4.74 for rat synaptophysin; see also 75), they have an additional charged residue in transmembrane domain 1 (E_{40}), another cysteine in transmembrane domain 2 (C_{130}), and, most importantly, they are completely different in their cytoplasmic end domains. While the amino termini do not share significant sequence homology, the characteristic cytoplasmic carboxy terminus of synaptophysin is absent in human and mouse pantophysin that have both only a short 26–amino acid end domain lacking the multiple tyrosine-containing motifs of synaptophysin and containing serines that are not embedded in typical phosphorylation consensus sites.

By alignment of the human, rat, and murine pantophysin cDNAs with the murine pantophysin gene sequence, the complete gene structure could be established identifying 6 exons that are interrupted by 5 introns of considerable size (Fig. 1). Remarkably, all 5 introns are located exactly at the corresponding positions in human and rat synaptophysin (Fig. 1; see also references 1, 54). On the other hand, pantophysin does not have a sixth intron which is present in the synaptophysin genes where it interrupts the 3′-noncoding region (Fig. 1).

Expression of Pantophysin mRNA in Neuroendocrine and Nonneuroendocrine Cells

Using the murine pantophysin cDNA clone bPM1 in Northern blot hybridization experiments, we analyzed the expression of pantophysin in various murine cell lines. Pantophysin mRNA could be identified under high stringency conditions in many different cell types including pluripotent embryonal stem cells, fibroblast-derived 3T3-L1 cells, and, most importantly, neuroendocrine pituitary tumor-derived AtT20 cells, although at a somewhat lower level (Fig. 2).

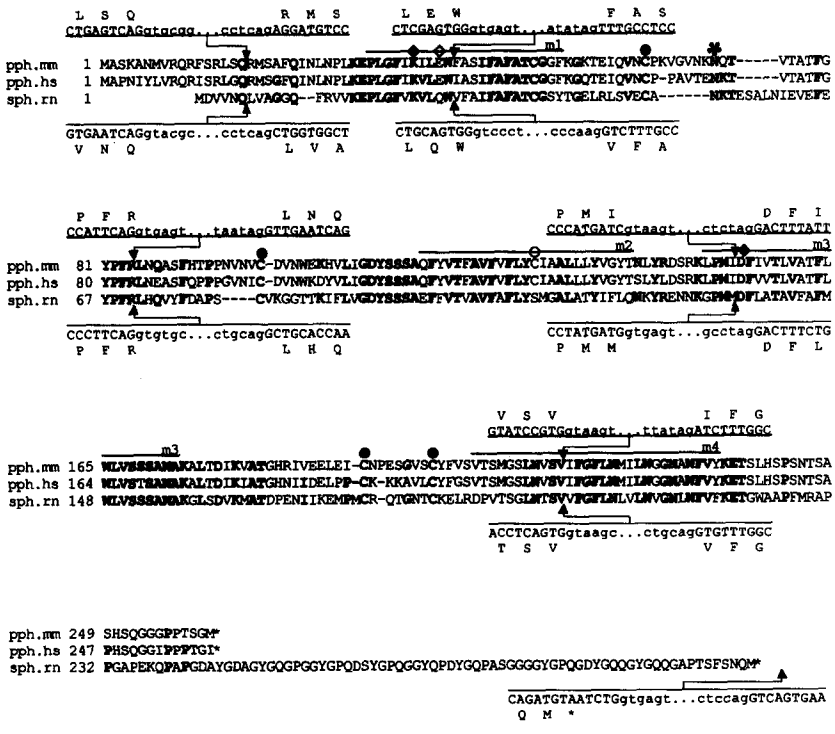

Figure 1. Comparison of the complete amino acid sequences of murine pantophysin (*pph.mm*), human pantophysin (*pph.hs*), and rat synaptophysin (*sph.rn*) as determined from the encoding genes (1; this study) or cDNA (40). Amino acids (one letter code; *, stop codons) conserved between either one or both of the pantophysins and synaptophysin are denoted by bold face letters and residue numbers given on the left. Potential transmembrane domains of high hydrophobicity are labeled as *m1*, *m2*, *m3*, and *m4*. The conserved N-glycosylation site is marked by a star, conserved charged residues in the transmembrane domains 1 and 3 by black diamonds, the charged residue present only in the transmembrane domain 1 of the pantophysins by a white diamond, the conserved cysteine residues in the intravesicular loops by black circles, and the cysteine residue present only in the transmembrane domain 2 of the pantophysins by a white circle. Intron positions and neighboring nucleotide sequences (*capital letters*, exons; *small letters*, introns) are shown to demonstrate the localization of introns 1-5 and of intron 6 that is only present in the 3′-noncoding region of rat synaptophysin.

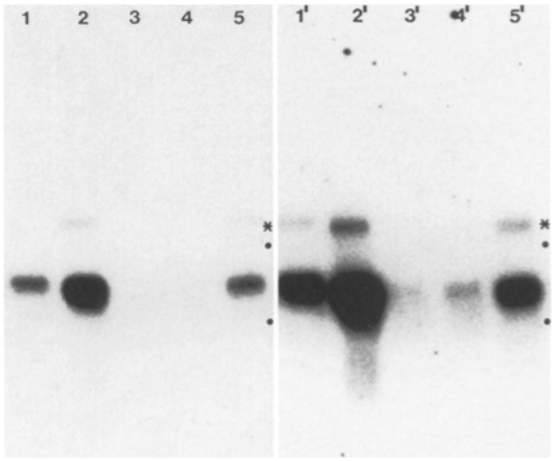

Figure 2. Autoradiographs of a Northern blot that was hybridized with a pantophysin-specific cRNA probe. Exposure was for 1 h at left, lanes *1–5*; and overnight at right, lanes *1'–5'*. RNAs were extracted from fibroblast-derived 3T3-L1 cells (20 μg total RNA, lanes *1* and *1'*; 20 μg poly(A)$^+$-RNA, lanes *2* and *2'*), pituitary tumor-derived AtT20 cells (20 μg total RNA, lanes *3* and *3'*; 20 μg poly(A)$^+$-RNA, lanes *4* and *4'*), and pluripotent embryonal stem cells of line R1 (20 μg poly(A)$^+$-RNA, lanes *5* amd *5'*). Note that pantophysin mRNA is not only detectable in non-neuroendocrine 3T3-L1 and R1 cells but also, after extended exposure, in neuroendocrine AtT20 cells (lanes 3' and 4'). The nature of the weaker reacting upper RNA (*) is not known. Positions of 28S and 18S RNAs are shown on the right margins (*dots*).

Intracellular Localization of Epitope-tagged Pantophysin in Transfected Cells

To examine the intracellular localization of pantophysin, constructs were prepared in which DNA fragments coding for defined epitopes were inserted in different regions of the pantophysin cDNA. After transfection of appropriate gene constructs into cultured cells transgene products were detected by immunofluorescence microscopy (Fig. 3). Typically, pantophysin was seen in multiple dotlike structures that were best resolved in the peripheral flat cytoplasm with increased staining near the plasma membrane of neighboring cells. Immunofluorescence was variable around the nucleus for all transfectants and ranged from partial caps, to circumferential crowns and dense regions covering the entire nucleus. The characteristic multipunctate localization, however, was the same for all constructs independent of the type of epitope tag (compare constructs PM1 with PS1 in Fig. 3, *c* and *e*) and of the position of the epitope tag (compare constructs MP1 and PM1 in Fig. 3, *b* and *c*). Even the addition of the long cytoplasmic carboxy-terminal extension of synaptophysin (cf. Fig. 1)

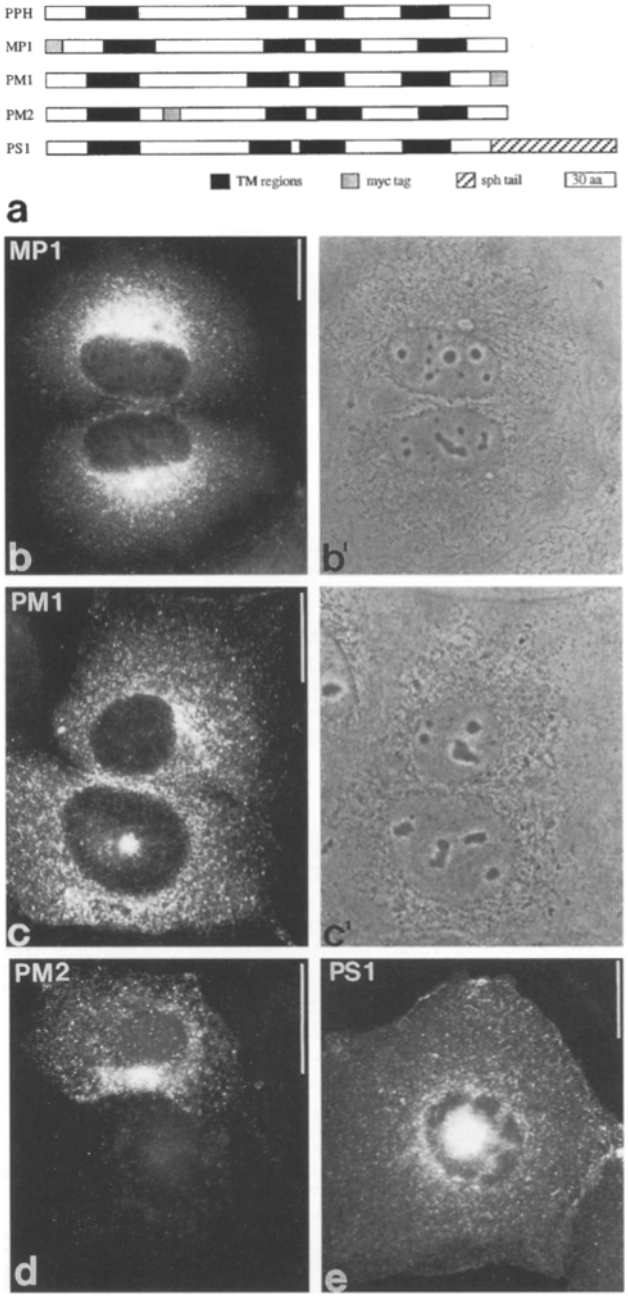

Figure 3. Immunofluorescence microscopy of hepatocellular carcinoma-derived PLC cells (methanol/acetone fixation) 3 d after transfection with cDNA constructs encoding epitope-tagged human pantophysin. The expressed polypeptides are drawn schematically in scale in *a* with the transmembrane domains in black, the myc epitope in gray, and the synaptophysin carboxy terminus in a diagonally striped pattern (protein denomination at left; wild-type pantophysin (*PPH*) is shown for comparison). (*b*) Immunofluorescence micrograph and corresponding phase contrast (*b'*) of two cells expressing MP1 after reaction with mAb MYC 1-9E10.2 detecting the myc epitope at the amino terminus of pantophysin. (*c*) Immunofluorescence microscopy and corresponding phase contrast (*c'*) of cells expressing PM1 that are stained by mAb MYC 1-9E10.2 detecting the myc epitope at the carboxy terminus of pantophysin. (*d*) Immunofluorescence of cells that were transfected with a construct coding for PM2 and were incubated with the myc antibody MYC 1-9E10.2 for 3 h before fixation and incubation with secondary antibodies only. Only the single transfected cell shown is strongly labeled. (*e*) Immunofluorescence microscopy of cells expressing PS1 that is detected by mAb SY38 detecting pantophysin fused to the cytoplasmic carboxy terminus of synaptophysin. Note that all transfected cells show a multipunctate cytoplasmic staining with variable labeling of the perinuclear region. Bars, 20 μm.

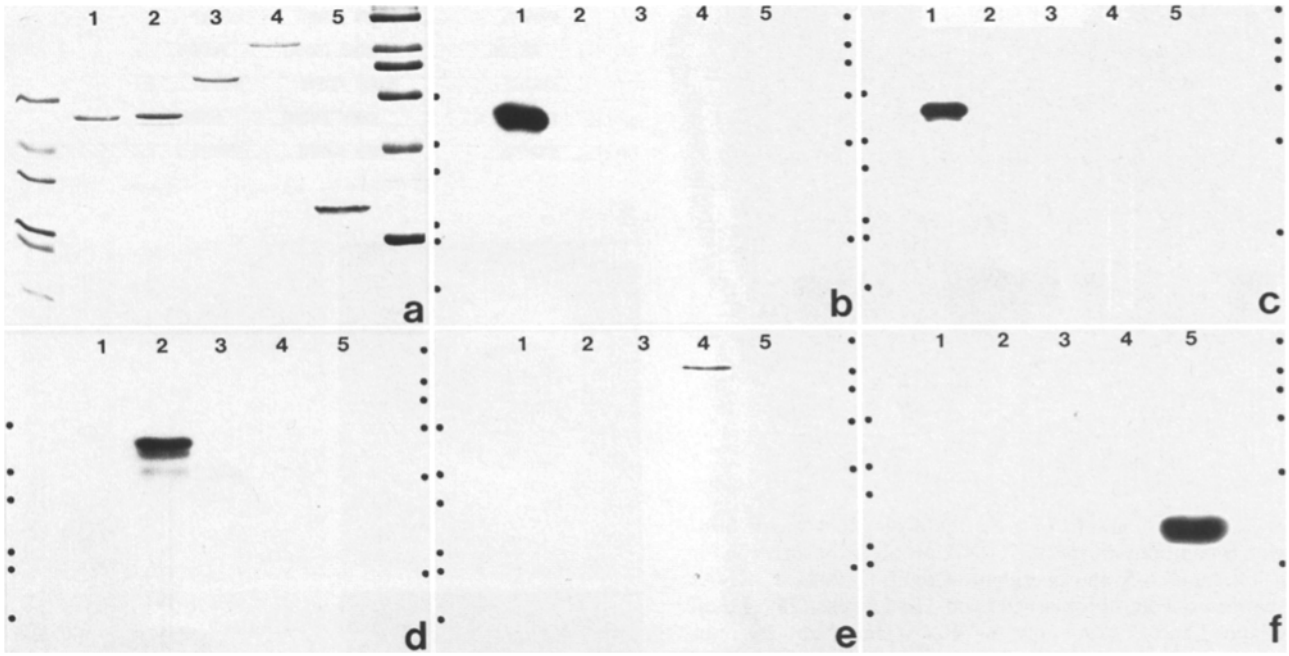

Figure 4. Immunoblot characterization of peptide antibodies against defined epitopes of pantophysin, synaptophysin, and synaptoporin. *a* shows Coomassie blue–stained polypeptides that were separated by 12% SDS-PAGE. Enriched fusion proteins produced in *E. coli* were loaded. They were synthesized from plasmids pETVP1 (lane *1*), coding for *Xenopus laevis* vimentin-1 with the cytoplasmic carboxy terminus of human pantophysin; pETPV2 (lane *2*), coding for the cytoplasmic amino terminus of human pantophysin fused to human vimentin; pET3ad.vimentin.GFP (lane *3*), coding for a chimera consisting of *Xenopus laevis* vimentin-1 and green fluorescent protein; pAX-GalS1 (lane *4*), coding for β-galactosidase with the cytoplasmic carboxy terminus of rat synaptophysin; and DHFR-HisPo4 (lane *5*), coding for dihydrofolate reductase with a poly-histidine tag and the cytoplasmic carboxy terminus of murine synaptoporin. The marker lanes contain the following polypeptides from top to bottom: at left BSA, M_r 66,000; ovalbumin, M_r 45,000; glyceraldehyde-3-phosphate dehydrogenase, M_r 36,000; carbonic anhydrase, M_r 29,000; trypsinogen, M_r 24,000; trypsin inhibitor, M_r 20,100; at right myosin heavy chain, M_r 205,000; β-galactosidase, M_r 116,000; phosphorylase b, M_r 97,400; BSA, M_r 66,000; ovalbumin, M_r 45,000; carbonic anhydrase, M_r 29,000. (*b–f*) Similar gels to that shown in *a* (corresponding lanes are labeled and positions of molecular mass markers are indicated by dots) were prepared and polypeptides were transferred onto nitrocellulose filters that were incubated with different antibodies: (*b*) affinity-purified antibodies from rabbit against the carboxy terminus of human pantophysin (peptide P-PHC2); (*c*) affinity-purified antibodies from chicken against the carboxy terminus of human pantophysin (peptide P-PHC3); (*d*) affinity-purified antibodies from rabbit against the amino terminus of human pantophysin (peptide P-PHN1); (*e*) mAb SY38 against the carboxy terminus of synaptophysin (for epitope mapping see reference 36); and (*f*) rabbit antibodies Cy^4 against synaptoporin (cf. 37). Specifically bound antibodies were detected using HRP-coupled secondary antibodies and an enhanced chemiluminescence system.

onto the entire pantophysin molecule did not affect the localization of the resulting chimeric molecule PS1 (Fig. 3 *e*). On the other hand, chimeras with transmembrane domains from both pantophysin and synaptophysin were not detectable in transfected cells under standard conditions, similar to the synaptophysin-connexin transmembrane chimeras described previously (41).

To test the predicted transmembrane topology of pantophysin, the myc epitope was inserted into the first intravesicular loop domain (construct PM2) that would be expected to be exposed to the cell surface if the molecule reached the plasma membrane during its life time. It was indeed possible to label transiently transfected cells by addition of antibodies to the culture medium resulting, again, in the characteristic multipunctate cytoplasmic staining (Fig. 3 *d*).

Pantophysin Protein Detection in Neuroendocrine and Nonneuroendocrine Tissues

To study pantophysin protein expression, antibodies were raised in chicken and rabbit against synthetic peptides corresponding to the unique cytoplasmically exposed end domains. These antibodies were shown to react specifically with the relevant pantophysin epitopes lacking cross reactivity with the corresponding domains of synaptophysin

Figure 5. Double label immunofluorescence of a 5-μm-thick, methanol/acetone-fixed cryosection of human pancreas detected by confocal laser scanning microscopy. *a* shows simultaneous detection of affinity-purified chicken antibodies against the carboxy-terminal peptide P-PHC3 of human pantophysin (*PPH*, red fluorescence) and rabbit antibodies against the cytoplasmic carboxy terminus of synaptophysin (*SPH*, green fluorescence). A strong immunoreactivity for pantophysin is only detectable in the exocrine portion, in blood vessel walls (*BV*), and surrounding connective tissue (*S*, stroma; *F*, fibroblast), whereas Langerhans islets are stained by both pantophysin and synaptophysin antibodies resulting in a yellow/orange color mixture. Partial colocalization is seen in individual nerve fibers (*N*). *b* and *c* show the individual recordings detecting pantophysin (*b*) or synaptophysin (*c*) that were used to create the image shown in *a*. Bars, 50 μm.

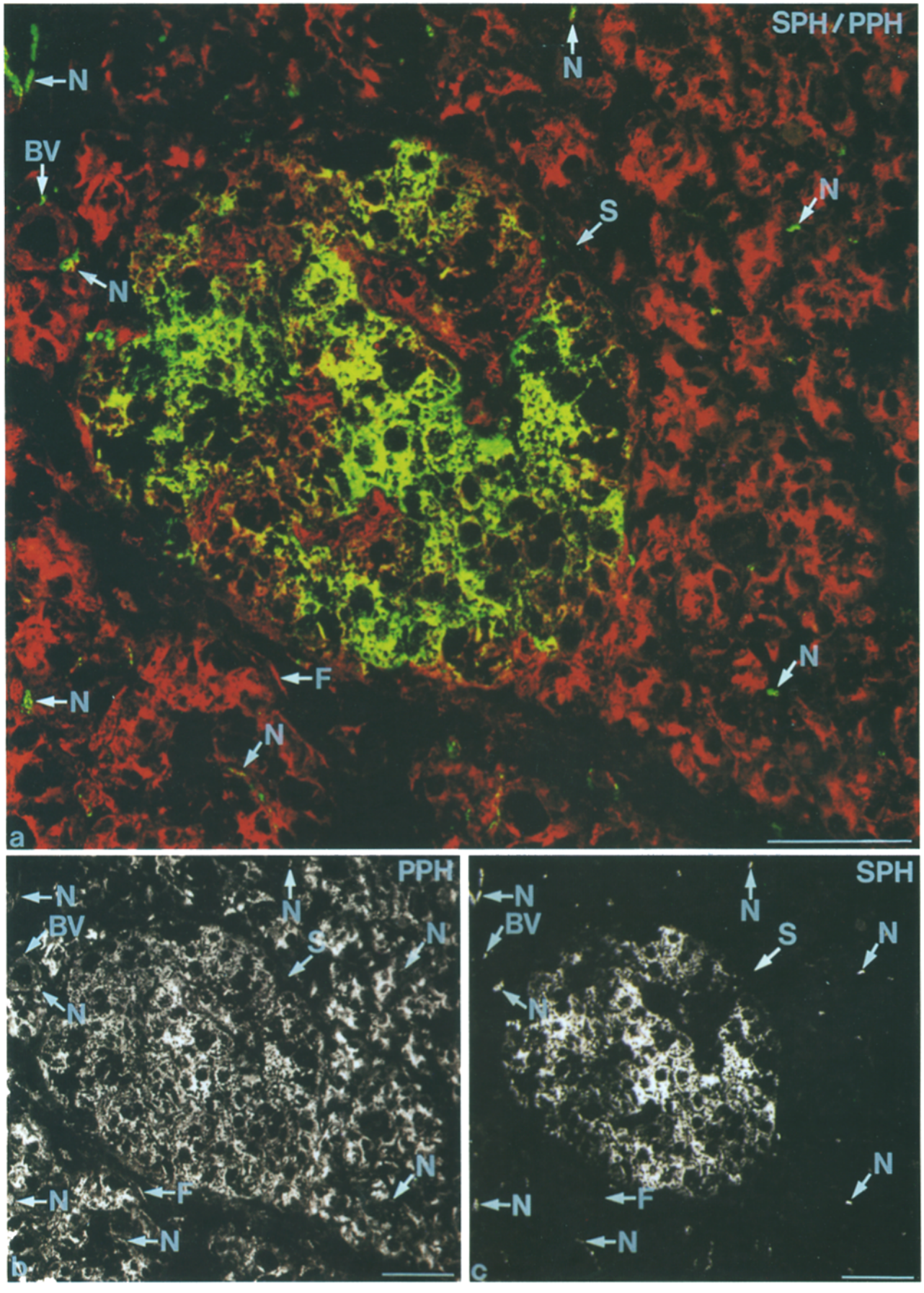
SPH / PPH
N
BV
S
F
a
PPH
b
SPH
c

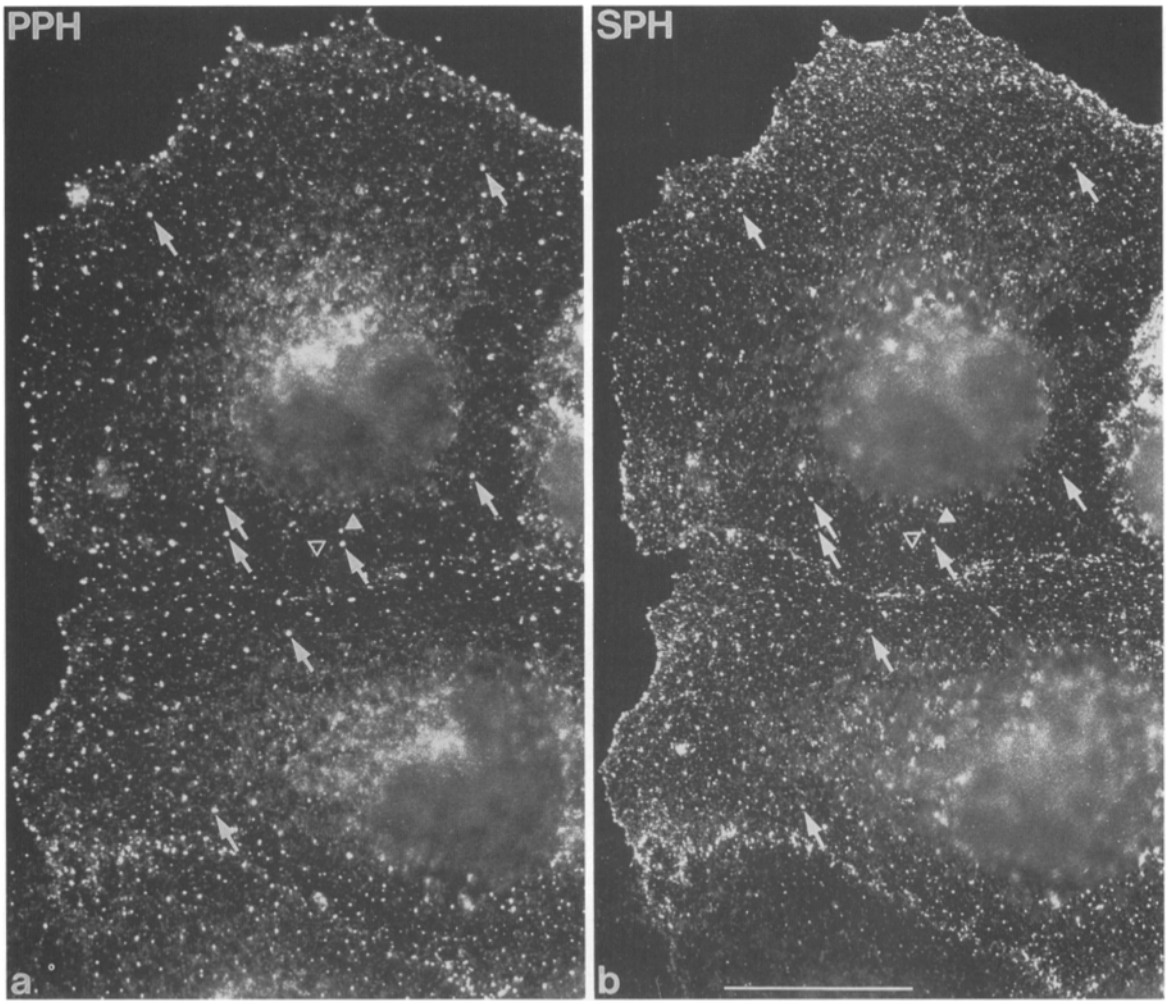

Figure 6. Double immunofluorescence microscopy of pantophysin (*PPH*, *a*) and synaptophysin (*SPH*, *b*) in cDNA-transfected synaptophysin-expressing PLC-derived subclone PLC-6S4. Cells were lysed with 0.25% saponin for 30 s and fixed with 2% formaldehyde for 30 min. Pantophysin was detected with affinity-purified chicken antibodies against the carboxy terminus of human pantophysin, synaptophysin with mAb SY38. Note the significant colocalization of both antigens at some structures (e.g., *arrows*) while others are only positive for either pantophysin (*solid arrowhead*) or synaptophysin (*open arrowhead*). Bar, 20 μm.

and synaptoporin (Fig. 4) and were used for the detection of pantophysin in tissues by immunofluorescence microscopy. Pancreas, as a tissue in which exocrine cells can be compared directly with endocrine cells, was examined in detail. Pantophysin staining was strongest in the exocrine portion (red in Fig. 5 *a*, corresponding single immunofluorescence recording in Fig. 5 *b*) and a weaker but still significant fluorescence was detectable in the neuroendocrine cells of Langerhans islets that also expressed synaptophysin (green in Fig. 5 *a*, single immunofluorescence in Fig. 5 *c*) thereby producing a yellow/orange color (Fig. 5 *a*). Nerve fibers were also positive for synaptophysin and pantophysin although synaptophysin immunoreactivity predominated. In addition, pantophysin antibodies reacted with blood vessel walls, including endothelial and myoid cells, and with connective tissue cells, while the extracellular space of the stroma was negative.

Pantophysin Colocalization with Cytoplasmic Vesicle Markers

To further characterize the pantophysin staining seen in tissue sections, immunofluorescence microscopy of cultured cells was performed. Detailed analyses of epithelial hepatocellular carcinoma-derived PLC cells, vulvar carcinoma-derived A431 cells, and certain subclones thereof showed that pantophysin was predominantly localized in dotlike structures in the cytoplasm and in a variable pat-

Figure 7. Double immunofluorescence microscopy of hepatocellular carcinoma-derived PLC cells after 0.25% saponin treatment (30 s), 2% formaldehyde fixation (30 min), and incubation with pantophysin antibodies (*PPH* in *a–d*; same antibodies as in Fig. 6 *a*) together with either affinity-purified rabbit peptide antibodies against β-COP (*a'*), mAb B3/25 against the transferrin receptor (*b*; *TFR*), mAb H4A3 against the lysosome-associated membrane protein 1 (*LAMP-1*) (*c'*), or mAb SG7C12 against secretory carrier-associated membrane proteins (*SCAMPs*) (*d'*). Note the partial colocalization of pantophysin and β-COP in the Golgi region in *a* and *a'*, the considerable

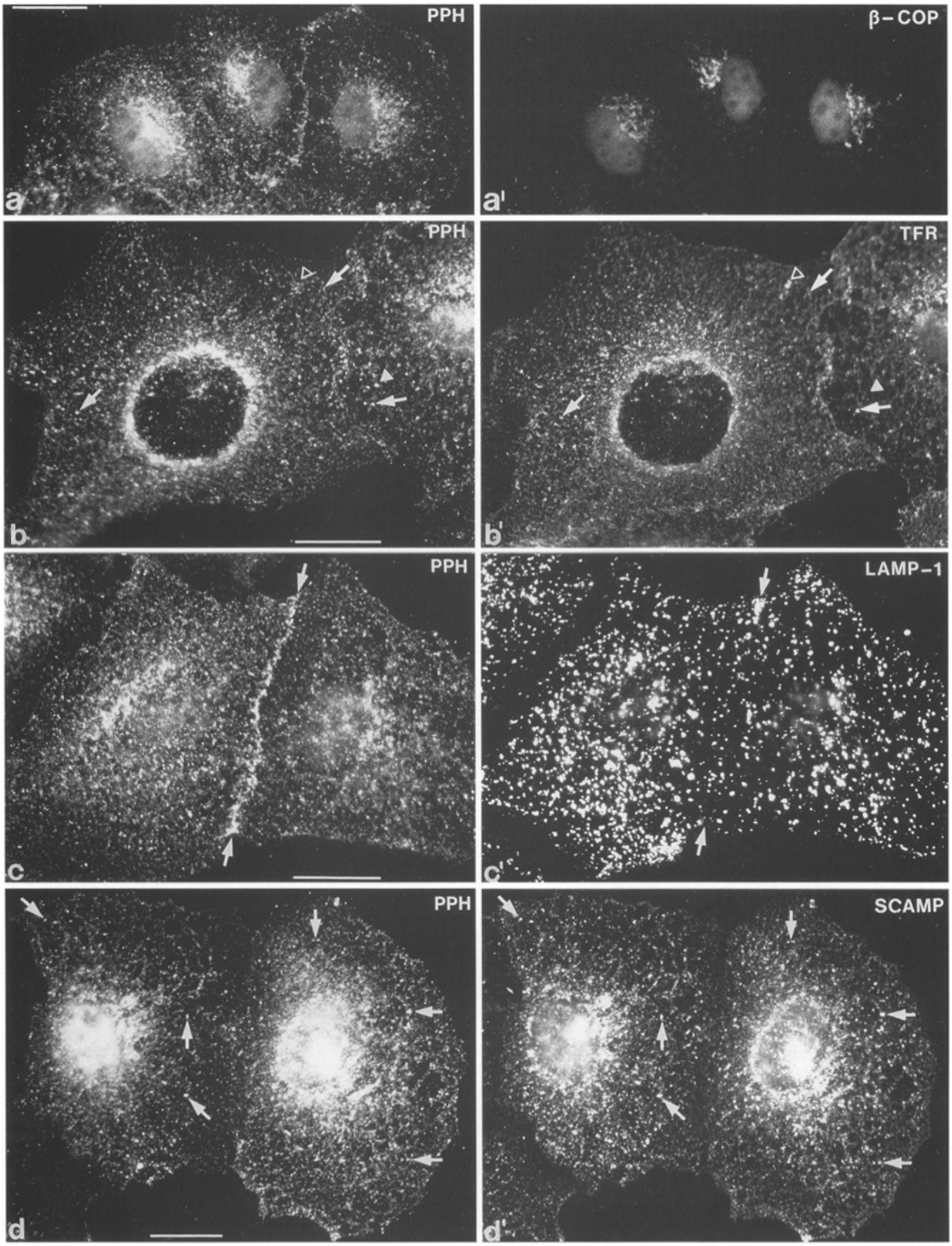

colocalization of pantophysin and the transferrin receptor in *b* and *b'* (*arrows*) besides significant differences (*solid arrowheads*, structures only labeled by pantophysin antibodies; *open arrowheads*, vesicles only labeled by transferrin receptor antibodies), the nonoverlapping distribution of pantophysin and LAMP-1 in *c* and *c'* with strong pantophysin staining at/or near the plasma membrane (*arrows*), and the significant colocalization of pantophysin and SCAMPs in *d* and *d'* (*arrows*). Bars, 20 μm.

tern around the nucleus similar to the epitope-tagged pantophysin in transfected cells (see Fig. 3).

Double label immunofluorescence microscopy of the recently established hepatocellular carcinoma-derived cell line PLC-6S4 and the vulvar carcinoma-derived subline A431-5S4, which both express synaptophysin in small cytoplasmic vesicles (44), showed that most of the pantophysin and synaptophysin immunoreactivities colocalized although at different relative intensities, and that a few structures were only labeled by either pantophysin or synaptophysin antibodies (Fig. 6; similar results were obtained in A431-5S4 cells). The examination of several epithelial cell lines such as PLC, A431, and mammary adenocarcinoma-derived MCF7 cells by double label immunofluorescence microscopy (representative results from PLC cells are shown in Fig. 7) revealed partial codistribution of pantophysin and the Golgi vesicle-associated protein β-COP in the juxtanuclear region (Fig. 7, *a* and *a'*; cf. 15). The variable perinuclear pantophysin staining (compare Fig. 3, *b–e*, Fig. 6 *a* and Fig. 7, *a–d*) may therefore, at least in part, be due to different orientations of the Golgi apparatus with respect to the nucleus in individual cells. Pantophysin also colocalized with the transferrin receptor, a marker for endocytotic recycling vesicles, although some "dots" were only positive for one or the other protein (Fig. 7, *b* and *b'*; cf. 44). The distribution of the lysosomal membrane proteins LAMP-1 and LAMP-2 was very different from that of pantophysin (Fig. 7, *c* and *c'*; cf. 41). Probably the best correlation was observed between the staining of pantophysin and SCAMPs, which are integral membrane proteins of secretory and cell surface recycling vesicles (Fig. 7, *d* and *d'*; see references 7, 8, 38). Furthermore, cellubrevin, a cellular homologue of the synaptic vesicle protein synaptobrevin (47), showed significant colocalization with pantophysin in A431 cells as well (Fig. 8, *a* and *b*) while the levels of cellubrevin expression in PLC cells were too low for immunofluorescence microscopic detection. Given all these observations, pantophysin staining overlapped with that of markers for certain small vesicles that participate in shuttling, secretion, endocytosis, and recycling.

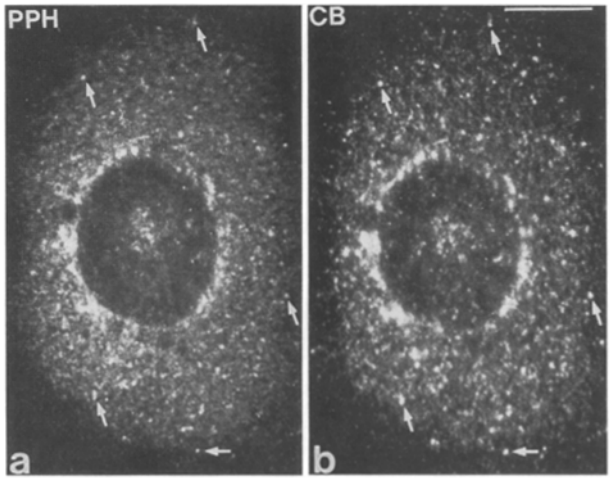

Figure 8. Double label immunofluorescence microscopy of methanol/acetone-fixed vulvar carcinoma-derived A431 cells detecting pantophysin (*PPH*) in (*a*) using affinity-purified chicken antibodies against the carboxy-terminal peptide P-PPHC3 of human pantophysin and cellubrevin (*CB*) in *b* using affinity-purified rabbit antibodies against the cytoplasmic amino terminus of cellubrevin that was produced in bacteria. Note the significant colocalization of individual puncta (e.g., *arrows*). Bar, 10 μm.

Immunoelectron Microscopic Detection of Pantophysin in Small, Electron-translucent Vesicles

By immunoelectron microscopy, the pantophysin-containing structures could be identified and different representative cellular regions are shown in Fig. 9. Abundant gold particles were seen associated with small, electron-translucent vesicles with a diameter between 40 and 70 nm (*arrows*). These smooth-surfaced vesicles were particularly abundant in regions of the cell periphery (Fig. 9 *c*) where practically all vesicles of this size category were labeled. The entire circumference, or only restricted surface domains of these vesicles, were decorated by immunogold (see especially high power magnifications in Fig. 9, *h–j*). Occasionally, restricted pantophysin labeling was also seen at circumscribed regions (less than 50 nm extension) of larger vesicles (*arrowheads*), multilamellar and multivesicular bodies (e.g., Fig. 9 *f*), Golgi apparatus (see, e.g., the Golgi-like cisterna in Fig. 9 *g*), peripheral ER regions (not shown), and plasma membrane (not shown). No immunolabel was associated with coated-pits and coated-vesicles (Fig. 9 *b*), mitochondria (Fig. 9 *d*), the nucleus (Fig. 9 *d*), or cytoplasmic filaments (Fig. 9, *e* and *j*).

Enrichment of Pantophysin in Transport Vesicles by Cell Fractionation

Pantophysin-positive vesicles could be enriched from A431 cells by differential centrifugation in different pellet

Figure 9. Immunoelectron microscopy of representative regions of vulvar carcinoma-derived A431 cells detecting pantophysin with affinity-purified chicken antibodies against the carboxy-terminal peptide P-PHC3 of human pantophysin and 5 nm gold-coupled secondary antibodies. *a–c* show areas that are either next to or close to the plasma membrane and are either transverse (*a* and *b*) or tangential sections (*c*). Note the presence of most gold particles around small 40–70-nm vesicles (*arrows*) and lack of label at cisternae of the rough endoplasmic reticulum (*ER*), the plasma membrane (*PM*), and coated pits (*CP*). A few larger vesicles (*arrowheads*) are also labeled. *d* shows cytoplasmic region next to the nucleus (*N*) with a single, strongly labeled small vesicle of 50 nm diameter (*arrow*; *inset*) together with gold particle-free membranes of the nuclear envelope (*NE*) and mitochondria (*M*). *e–g* depict cytoplasmic areas containing variously shaped vesicles and membranes. Note that in each micrograph small 40–70-nm vesicles are labeled by immunogold (*arrows*) but restricted regions of some larger vesicles (*arrowheads*) and multivesicular bodies (*MV*; labeled region denoted by > in *f*) are decorated by gold particles. Endoplasmic reticulum (*ER*) and Golgi cisternae (*GA*) are negative except for limited areas (e.g., region in *g* denoted by >), and no label is seen at cytoskeletal elements including intermediate filaments (*IF*). *h–j* are high power magnifications demonstrating characteristics of the small 40–70 nm electron translucent vesicles (*arrows*) that are either circumferentially labeled or only decorated by gold particles in a caplike fashion. The few larger vesicles (*arrowheads*) are decorated with immunolabel only at restricted surface domains. *IF*, intermediate filaments. Bars, (*a–h*) 500 nm; (*i–k*) and inset in *d*, 50 nm.

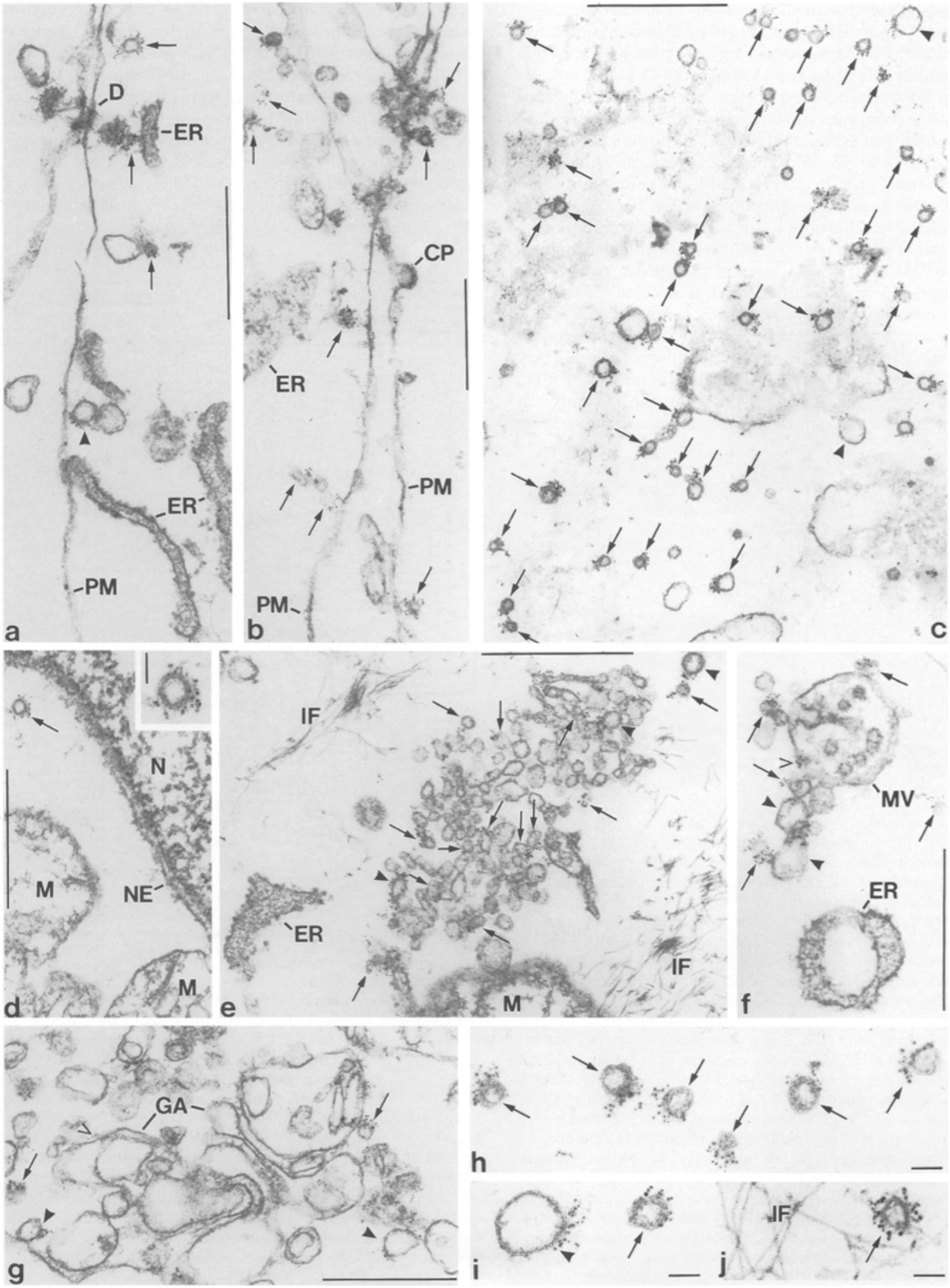
D
ER
ER
PM
a
CP
ER
PM
PM
b
c
N
M
NE
M
d
IF
ER
M
IF
e
MV
ER
f
GA
g
h
i
IF
j

fractions (P1–P4) with the most significant accumulation in a 100,000 *g* pellet (P4 in Fig. 10 *a*). Pantophysin immunoreactivity was detected as a variable pattern of multiple bands in the molecular mass range of 36–45 kD, characteristic of an N-glycosylated protein with differentially processed carbohydrate moieties (for different electrophoretic mobility of synaptophysin see for example references 34, 35, 39, 43, 50, 75, 76). When these pellet fractions were treated with Triton X-100 practically all pantophysin could be solubilized (prolonged exposure in Fig. 10 *b*).

To characterize pantophysin vesicles in a cell type that expresses synaptophysin constitutively, myc-tagged pantophysin PM1 (cf. Fig. 3) was expressed in neuroendocrine PC12 cells. Cell clone PC12-PM3 was selected for analysis on the basis of its strong cytoplasmic immunofluorescence with myc antibodies (not shown). Although no reproducible signal was obtained by immunoblotting, an ELISA could be developed that allowed the detection of myc-tagged pantophysin. Using this assay it was shown that a large percentage of pantophysin immunoreactivity cosedimented with synaptophysin-containing vesicles in equilibrium or velocity gradient centrifugation (Fig. 11; specific density of peak fraction 7 in Fig. 11 *a* ~1.111 g/l).

The composition of pantophysin vesicles was then analyzed by immunoisolation experiments. To improve the detectability of the low amounts of endogenous pantophysin, A431 cells were stably transfected with a myc-tagged pantophysin version (PM1; cf. Fig. 3) that also reacted with our pantophysin antibodies, together with a synaptophysin gene construct. Vesicles immunoisolated with pantophysin antibodies from these doubly transfected,

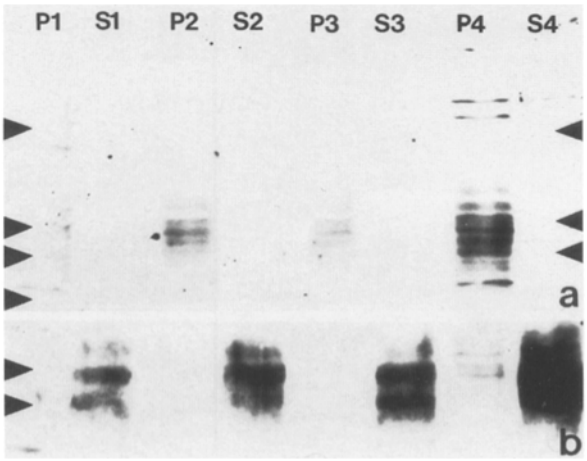

Figure 10. Immunoblots of different cell fractions obtained from PLC-6S4 cells that were stably transfected with a synaptophysin cDNA construct. Cells were lysed in hypotonic buffer (H buffer) and homogenized before consecutive differential centrifugation at 1,000 *g*, 7,000 *g*, 15,000 *g*, and 100,000 *g* resulting each time in a pellet (*P1*, *P2*, *P3*, and *P4*) and supernatant (*S1*, *S2*, *S3*, and *S4*). Approximately equal amounts of protein were loaded in each lane, transferred onto nitrocellulose membranes, and incubated with affinity-purified antibodies against the cytoplasmic carboxy terminus of human pantophysin. Bound antibodies were detected with the help of an enhanced chemiluminescence system. Arrowheads on both margins show the positions of coelectrophoresed molecular mass markers BSA (M_r 66,000), ovalbumin (M_r 45,000), glyceraldehyde-3-phosphate dehydrogenase (M_r 36,000), and carbonic anhydrase (M_r 29,000; not shown at right). The weak upper bands in P4 are probably multimeric aggregates. Note that most pantophysin immunoreactivity is seen in the 100,000-*g* pellet (*P4*). (*b*) Pellet fractions P1–P4 were incubated overnight in H buffer containing 1% Triton X-100 and were recentrifuged at 100,000 *g* resulting in pellets P1′–P4′ and supernatants S1′–S4′ that were also subjected to immunoblotting with pantophysin antibodies as in *a* (same loading scheme). Positions of molecular mass markers ovalbumin (M_r 45,000) and glyceraldehyde-3-phosphate dehydrogenase (M_r 36,000) are shown on the left margin. Note that even in the prolonged exposure practically all pantophysin is now detected in the soluble supernatant fractions.

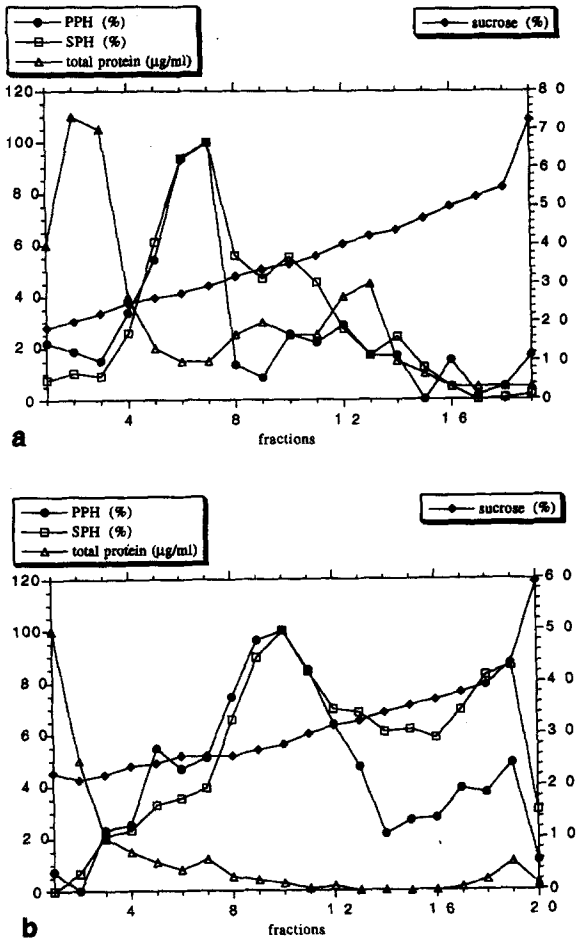

Figure 11. Detection of pantophysin and synaptophysin in sucrose gradient fractions of rat pheochromocytoma-derived neuroendocrine PC12 cells stably expressing myc-tagged pantophysin PM1 (cf. Fig. 3) by ELISA. Postnuclear supernatants were loaded on top of linear sucrose gradients (15%–60% in *a* and 15%–45% in *b*), each with a 70% sucrose cushion at the bottom, and centrifuged for either 17.5 h at 140,000 *g* (*a*) or for 160 min at 270,000 *g* (*b*). Fractions were collected from top to bottom (left to right on abscissa). Sucrose concentration was measured with an Abbé refractometer (*filled squares*; scale on right ordinate in wt/vol %), protein concentration was determined with the help of the colorimetric BioRad assay (*triangles*; scale on left ordinate in µg/ml), and immunoreactivities of either mAb SY38 detecting synaptophysin (*open squares*) or mAb MYC 1-9E10.2 reacting with myc-tagged human pantophysin PM1 (*circles*) were measured by ELISA and are given as relative percentages of the maximal value set as 100% (scale on left ordinate). Note the codistribution of the major immunoreactivities of both antigens.

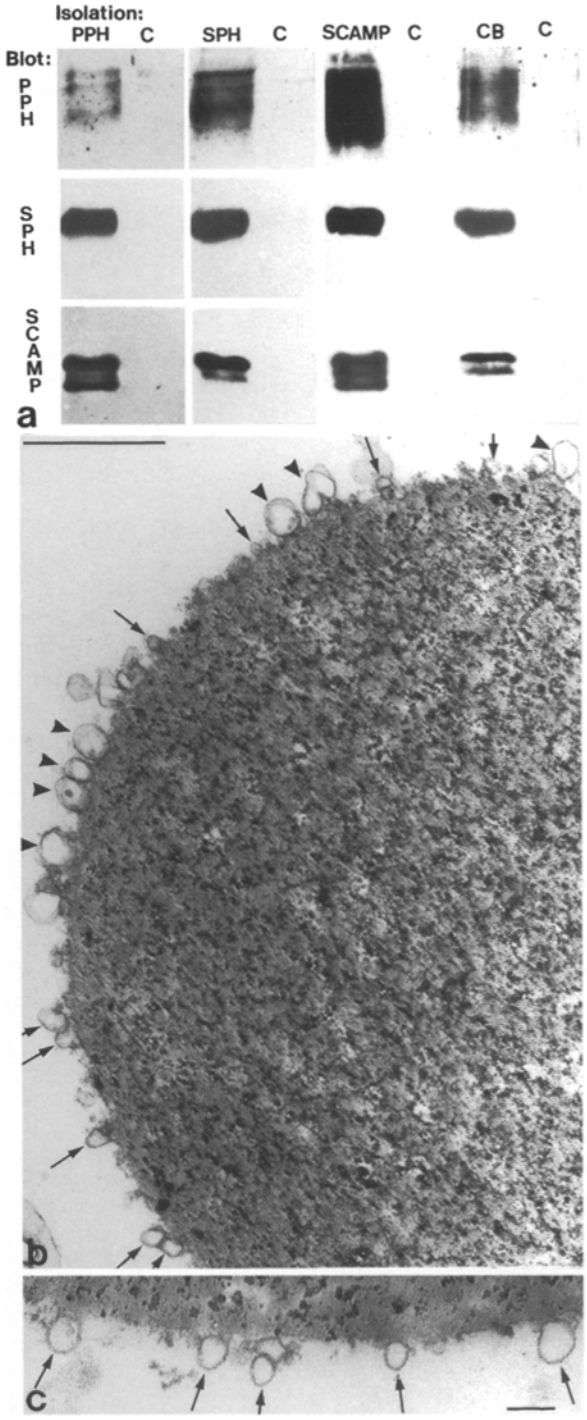

Figure 12. Immunoblots (*a*) and electron microscopy (*b* and *c*) of vesicles that were immunoisolated from 15,000 *g* supernatants obtained from wild-type A431 cells (*c*) or A431 subclone A6S4PM18 stably expressing synaptophysin and myc-tagged pantophysin PM1 (*a* and *b*). (*a*) Immunoblots of gel electrophoretically separated (SDS-PAGE) cell fractions that were immunoisolated with antibodies against pantophysin (*PPH*; affinity-purified antibodies against the carboxy terminus), synaptophysin (*SPH*; mAb SY38), secretory carrier-associated membrane proteins (*SCAMP*; mAb SG7C12), and cellubrevin (*CB*; affinity-purified antibodies against the cytoplasmic amino terminus) or only with secondary antibodies (*C*), and were subsequently blotted with the same antibodies in different combinations as indicated. (*b* and *c*) Electron micrographs show that the material immunoisolated with pantophysin antibodies consists mostly of small diameter vesicles (40–70 nm; *arrows*) and several larger vesicles (*arrowheads* in *b*). Bars: (*b*) 500 nm; (*c*) 100 nm.

stable cells (clone A6S4PM18) contained synaptophysin, SCAMPs (Fig. 12 *a*, *left column*), and cellubrevin (not shown). Fig. 12 *b* shows immunoadsorbed vesicles from A6S4PM18 cells that were similar to those isolated from wild-type A431 cells (Fig. 12 *c*). Conversely, pantophysin could be copurified in immunoisolation experiments using antibodies against synaptophysin, SCAMPs, and cellubrevin (Fig. 12 *a*, *upper row*).

Finally, the distribution of pantophysin and synaptophysin was investigated in vivo in a human pheochromocytoma as a neuroendocrine tumor known to express large amounts of synaptophysin (see for example reference 76). Strongly synaptophysin-positive tumor islets were, however, only weakly or not at all labeled by pantophysin antibodies (Fig. 13, *a–c*). Yet, immunoisolation experiments using antibodies against either synaptophysin or pantophysin demonstrated unequivocally that a certain proportion of synaptophysin and pantophysin molecules must be present in the same vesicles of the 15,000-*g* supernatants (Fig. 13 *d*) as is also the case for the PC12 subline PC12-PM3 that overexpressed myc-tagged pantophysin (Fig. 13 *e*; see also Fig. 11). But it was not possible to immunodeplete the starting fractions completely of synaptophysin using pantophysin antibodies, or of pantophysin using synaptophysin antibodies even under optimized conditions indicating that some of the vesicles contain only either one or the other molecule.

Discussion

We showed that the synaptophysin homologue pantophysin is a ubiquitously expressed integral membrane protein of a certain type of cytoplasmic vesicle. The typical pantophysin vesicles have a diameter of <100 nm (average 40–70 nm), a smooth surface and an electron-translucent lumen. By these criteria they are indistinguishable from transport vesicles that have been described in various intracellular shuttling pathways (4, 14, 28, 48, 51–53). This interpretation is also supported by double label immunofluorescence microscopy and immunoisolation experiments showing that pantophysin codistributes with membrane markers for such vesicles present in the Golgi region, the transferrin receptor-positive recycling system connecting the plasma membrane and endosomes, and in ubiquitous secretory and endocytotic pathways that are characterized by the presence of the cellular vSNARE cellubrevin and the secretory carrier-associated membrane proteins (SCAMPs) (Figs. 7, 8, and 12). Interestingly, synaptophysin and pantophysin colocalize in the same small cytoplasmic vesicles in transfected nonneuroendocrine and neuroendocrine cells and in neuroendocrine tissues (e.g., Figs. 6, 11, 12, and 13; for pantophysin mRNA expression in neuroendocrine and neuronal cells see also reference 40). We conclude therefore that pantophysin is a marker for small cytoplasmic transport vesicles independent of their cargo in many cell types, and thereby represents a common property of all these different vesicles for which it probably fulfills basic structural and housekeeping functions.

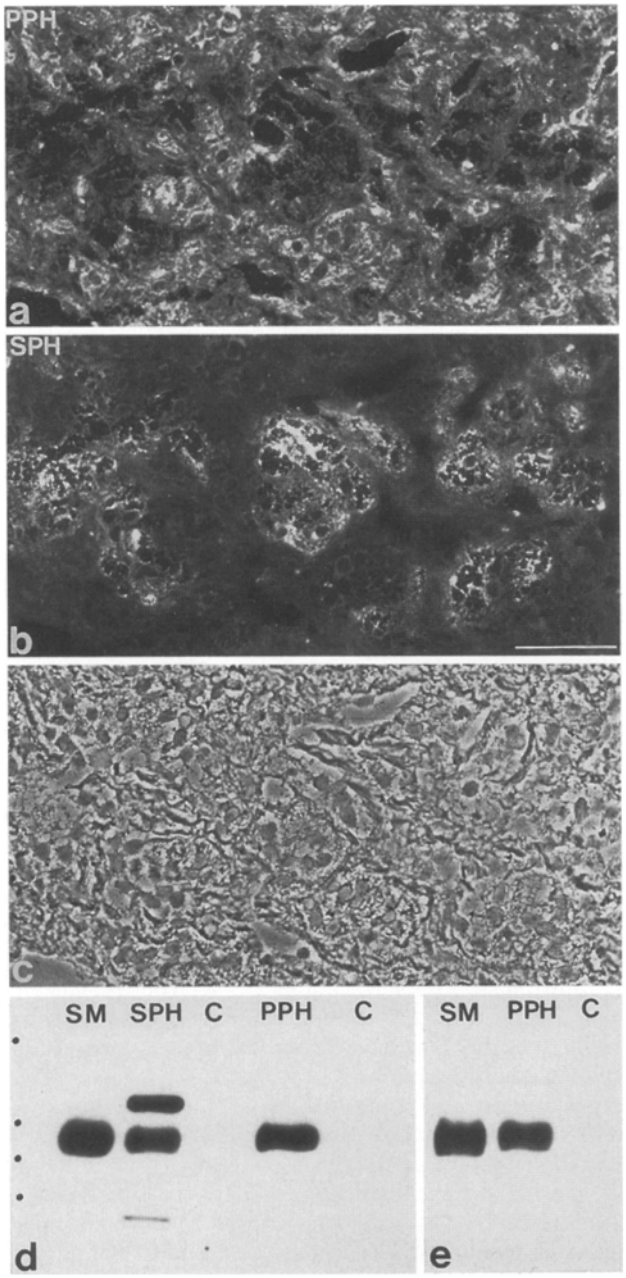

Figure 13. Colocalization of pantophysin and synaptophysin by immunofluorescence microscopy (*a–c*) and immunoblotting of immunoisolates (*d* and *e*) of a human pheochromocytoma (*a–d*) and the rat pheochromocytoma-derived cell line PC12-PM3 (*e*). *a–c* shows double immunofluorescence microscopy and corresponding phase contrast (*c*) detecting pantophysin (*PPH*; *a*) using affinity-purified antibodies from chicken against the carboxy-terminal peptide P-PHC3 of human pantophysin and mAb SY38 directed against synaptophysin (*SPH*; *b*). Note that pantophysin is expressed in most cells with significantly reduced levels in the strongly synaptophysin-positive tumor islets. Bar, 50 μm. (*d*) Immunoblot of cell fractions and vesicles that were isolated from 15,000 *g* supernatants obtained from the human pheochromocytoma shown in *a–c*. Polypeptides were separated by 12% SDS-PAGE, and synaptophysin was detected on immunoblots using mAb SY38 and an enhanced chemiluminescence system. Lane *SM* contains the 15,000-*g* supernatant starting material (45 μg total protein); lane *SPH* contains material isolated with mAb SY38-coupled magnetic beads as positive control (the upper ~53-kD and lower ~23-kD bands are due to reaction of the secondary antibodies with the heavy and light chains of SY38) next to lane *C* with material isolated with magnetic beads coated only with secondary rat anti-mouse IgG1 antibodies as negative control; lane *PPH* vesicles are isolated with magnetic beads coupled to affinity-purified chicken antibodies against the carboxy terminal peptide P-PHC3 of human pantophysin (~10 times more material was loaded than in lane *SPH*) next to lane *C* with material isolated with magnetic beads coated only with secondary rabbit anti-chicken IgY antibodies. Note that synaptophysin-containing vesicles can be immunoisolated with pantophysin antibodies. (*e*) Immunoblot of cell fractions and vesicles obtained from PC12 subclone PC12-PM3 (*e*) expressing the myc-tagged pantophysin version PM1 (see also Figs. 3 and 11) after reaction with synaptophysin mAb SY38 (same procedure as in *d*). Lane *SM* shows the 15,000-*g* starting material (20 μg total protein), lane *PPH* vesicles immunoisolated with the help of magnetic beads coupled to mAb MYC 1-9E10.2 against the myc epitope present in the transgenic pantophysin, and lane *C* material isolated with magnetic beads coated with secondary antibodies only. Compare the results with those shown in *d*. The relative position of the coelectrophoresed size markers for *d* and *e* are indicated by dots at left (*from top to bottom*) BSA (M_r 66,000), ovalbumin (M_r 45,000), glyceraldehyde-3-phosphate dehydrogenase (M_r 36,000), and carbonic anhydrase (M_r 29,000).

In our immunoelectron microscopical examinations, we rarely saw vesicles in a state of budding or docking, possibly due to the comparatively short time period of these events during the life time of a carrier vesicle. Epitope masking may be another plausible reason for this lack of detection due to altered conformation of the antigen or to reduced accessibility of the antibody. This could also explain why pantophysin was never detected in coated-vesicles and -pits (for synaptophysin-epitope masking in clathrin-coated vesicles see reference 46). The small clusters of pantophysin immunogold particles which were seen in restricted regions of ER, Golgi apparatus, multivesicular bodies, and plasma membrane could therefore be the result of previous vesicle fusion events or indicate immanent vesicle fission at these locations. Considering the strong and direct interaction of synaptophysin with v SNAREs of the synaptobrevin type (11, 16, 72), it will be of interest to find out whether pantophysin interacts with the widely expressed synaptobrevin isoform cellubrevin that we have shown to be present in pantophysin vesicles (Figs. 8 and 12), thereby regulating membrane fusion events.

We have also provided compelling evidence that pantophysin is a member of the synaptophysin family by showing similarities in gene structure and amino acid sequence (see also references 40, 77). The high degree of conservation of the transmembrane domains and connecting intravesicular loops suggests that these regions are essential for basic properties common to all family members while the divergent cytoplasmic end domains of synaptophysin are important for certain aspects of regulated exocytosis in neurons. Clearly, the end domain of synaptophysin is neither needed for intracellular topogenesis (41) nor does it alter the localization of pantophysin in transfected cells as shown by our chimera PS1 that consists of the entire pantophysin molecule linked to the cytoplasmic carboxy terminus of synaptophysin (Fig. 3).

We showed that the expression of the synaptophysin

isoform pantophysin is not restricted to a particular cell type but defines a ubiquitous vesicle of similar size and appearance as the typical synaptophysin-positive vesicle in neurons and neuroendocrine cells (for example see references 50, 75). Isoforms of several other synaptic vesicle proteins have also been identified that are expressed in nonneuroendocrine cells (e.g., 7–10, 22, 24, 32, 45, 47, 58–60, 63, 71). For example, isoforms of the vSNARE synaptobrevin have been shown to colocalize with transferrin-containing recycling vesicles in fibroblasts (24, 47), with vesicles in the ER/Golgi region of skeletal muscle (58, 71), with zymogen granules of exocrine cells and dense core vesicles of β cells in pancreas (9, 59), with glucose transporter–containing vesicles in adipocytes (10), or water channels in the collecting ducts of kidney (22). Conversely, SCAMPs are not only constituents of secretory and endocytotic vesicles in nonneuroendocrine cells but also of synaptic vesicles (7, 8, 38). Expression of the individual family members is not mutually exclusive (see for example Fig. 5) and our finding that pantophysin and synaptophysin can even colocalize in the same vesicle (Figs. 12 and 13) is paralleled by the observed codistribution of synaptophysin and synaptoporin (23), of cellubrevin and synaptobrevins (12), or of Rab3A and Rab5 (21) in the same vesicles suggesting overlapping functions of the different family members (see also references 45, 70), a notion that is also supported by the lack of dramatic defects in synaptophysin-deficient mice (17) in which pantophysin might substitute for synaptophysin.

The presence of other polypeptides with four membrane-spanning domains such as the SCAMPs and synaptogyrins in synaptic vesicles (3, 7, 8, 64) and, at least in the case of the SCAMPs, in ubiquitous pantophysin-containing cytoplasmic vesicles of nonneuroendocrine cells (this study; see also references 7, 8, 38) adds a further degree of complexity and potential functional redundancy. Although there is no resemblance in primary amino acid sequence between these different gene families there are characteristic features shared by all the encoded molecules such as the same transmembrane topology with amino- and carboxy-termini facing the cytoplasm, and the tendency to form homooligomers (8, 23, 34, 64, 68) formally shown only for synaptophysin and synaptoporin (23, 34, 68). It is possible that all these molecules perform similar basic functions that are important for membrane domain biogenesis and maintenance including regulation of vesicle fusion and intravesicular milieu as well (for possible functions of synaptophysin see references 11, 16, 25, 62, 68, 72). Different stoichiometric combinations of these polypeptides could confer specific properties to a given membrane in a given cell. We have proposed, in the case of synaptophysin, that it is a major structural determinant of small cytoplasmic vesicles (39, 43, 44) and related molecules such as pantophysin could also be important for formation and/or maintenance of these membranes with high curvature (see also reference 64).

We wish to thank Judith Rudisile, Anke Marschall, and Stephanie Heupel for engaged and valuable technical assistance; Jutta Müller-Osterholt for technical help with photography; Uwe Leimer for helpful suggestions; Drs. David Castle (University of Virginia, Charlottesville, VA), Heinrich Betz (Max-Planck-Institute, Frankfurt, FRG), Rainer Duden, and Thomas Kreis (then at EMBL, Heidelberg, FRG) for antibodies; Dr. Harald Herrmann for provision of vimentin cDNA clones; Dr. Herbert Spring for help with confocal Laser Scan Microscopy; Drs. Hans-Richard Rackwitz and Doris Schiller-Gramlich for synthesis and purification of oligopeptides; and Dr. Werner Franke for support and encouragement. The murine pantophysin sequence has been submitted to the GenBank and is available under the accession number US8869.

This work was supported by the German Research Council (SFB 317).

Received for publication 7 March 1996 and in revised form 29 April 1996.

References

1. Bargou, R.C.E.F., and R.E. Leube. 1991. The synaptophysin-encoding gene in rat and man is specifically transcribed in neuroendocrine cells. *Gene (Amst.).* 99:197–204.
2. Barlowe, C., L. Orci, T. Yeung, M. Hosobuchi, S. Hamamoto, N. Salama, M.F. Rexach, M. Ravazzola, M. Amherdt, and R. Schekman. 1994. COP II: a membrane coat formed by Sec proteins that drive vesicle budding from the endoplasmic reticulum. *Cell.* 77:895–907.
3. Baumert, M., K. Takei, J. Hartinger, P.M. Burger, G. Fischer von Mollard, P.R. Maycox, De Camilli, P., and R. Jahn. 1990. p29: a novel tyrosine-phosphorylated membrane protein present in small clear vesicles of neurons and endocrine cells. *J. Cell Biol.* 110:1285–1294.
4. Bednarek, S.Y., M. Ravazzola, M. Hosobuchi, M. Amherdt, A. Perrelet, R. Schekman, and L. Orci. 1995. COPI- and COPII-coated vesicles bud directly from the endoplasmic reticulum in yeast. *Cell.* 83:1183–1196.
5. Bennett, M.K., and R.H. Scheller. 1993. The molecular machinery for secretion is conserved from yeast to neurons. *Proc. Natl. Acad. Sci. USA.* 90:2559–2563.
6. Bennett, M.K., and R.H. Scheller. 1994. A molecular description of synaptic vesicle membrane trafficking. *Annu. Rev. Biochem.* 63:63–100.
7. Brand, S.H., S.M. Laurie, M.B. Mixon, and J.D. Castle. 1991. Secretory carrier membrane proteins 31-35 define a common protein composition among secretory carrier membranes. *J. Biol. Chem.* 266:18949–18957.
8. Brand, S.H., and J.D. Castle. 1993. SCAMP 37, a new marker within the general cell surface recycling system. *EMBO (Eur. Mol. Biol. Organ.) J.* 12:3753–3761.
9. Braun, J.E.A., B.A. Fritz, S.M.E. Wong, and A.W. Lowe. 1994. Identification of a vesicle-associated membrane protein (VAMP)-like membrane protein in zymogen granules of the rat exocrine pancreas. *J. Biol. Chem.* 269:5328–5335.
10. Cain, C.C., W.S. Trimble, and G.E. Lienhard. 1992. Members of the VAMP family of synaptic vesicle proteins are components of glucose transporter-containing vesicles from rat adipocytes. *J. Biol. Chem.* 267: 11681–11684.
11. Calakos, N., and R.H. Scheller. 1994. Vesicle-associated membrane protein and synaptophysin are associated on the synaptic vesicle. *J. Biol. Chem.* 269:24534–24537.
12. Chilcote, T.J., T. Galli, O. Mundigl, L. Edelmann, P.S. McPherson, K. Takei, and P. De Camilli. 1995. Cellubrevin and synaptobrevins: similar subcellular localization and biochemical properties in PC12 cells. *J. Cell Biol.* 129:219–231.
13. Dent, J.A., R.B. Cary, J.B. Bachant, A. Domingo, and M.W. Klymkowsky. 1992. Host cell factors controlling vimentin organization in the Xenopus oocyte. *J. Cell Biol.* 119:855–866.
14. de Curtis, I., and K. Simons. 1989. Isolation of exocytic carrier vesicles from BHK cells. *Cell.* 58:719–727.
15. Duden, R., G. Griffith, R. Frank, P. Argos, and T.E. Kreis. 1991. β-COP, a 110 kD protein associated with non-clathrin-coated vesicles and the Golgi complex, shows homology to β-adaptin. *Cell.* 64:649–665.
16. Edelmann, L., P.I. Hanson, E.R. Chapman, and R. Jahn. 1995. Synaptobrevin binding to synaptophysin: a potential mechanism for controlling the exocytotic fusion machine. *EMBO (Eur. Mol. Biol. Organ.) J.* 14:224–231.
17. Eshkind, L.G., and R.E. Leube. 1995. Mice lacking synaptophysin reproduce and form typical synaptic vesicles. *Cell Tissue Res.* 282:423–433.
18. Evan, G.I., G.K. Lewis, G. Ramsay, and W.A. Rutter. 1985. Isolation of monoclonal antibodies specific for human c-*myc* protooncogene product. *Mol. Cell. Biol.* 5:3610–3616.
19. Farquhar, M.G. 1985. Progress in unraveling pathways of Golgi traffic. *Annu. Rev. Cell Biol.* 1:447–488.
20. Ferro-Novick, S., and R. Jahn. 1994. Vesicle fusion from yeast to man. *Nature (Lond.).* 370:191–193.
21. Fischer von Mollard, G., B. Stahl, C. Walch-Solimena, K. Takei, L. Daniels, A. Khoklatchev, P. De Camilli, T.C. Südhof, and R. Jahn. 1994. Localization of Rab5 to synaptic vesicles identifies endosomal intermediate in synaptic vesicle recycling pathway. *Eur. J. Cell Biol.* 65:319–326.
22. Franki, N., F. Macaluso, W. Schubert, L. Gunther, and R.M. Hays. 1995. Water channel-carrying vesicles in the rat IMCD contain cellubrevin. *Am. J. Physiol.* 269:C797–801.
23. Fykse, E.M., K. Takei, C. Walch-Solimena, M. Geppert, R. Jahn, P. De Camilli, and T.C. Südhof. 1993. Relative properties and localization of synaptic vesicle protein isoforms: the case of the synaptophysins. *J. Neurosci.* 13:4997–5007.

24. Galli, T., T. Chilcote, O. Mundigl, T. Binz, H. Niemann, and P. De Camilli. 1994. Tetanus toxin-mediated cleavage of cellubrevin impairs exocytosis of transferrin receptor-containing vesicles in CHO cells. *J. Cell Biol.* 125: 1015–1024.
25. Galli, T., P.S. McPherson, and P. De Camilli. 1996. The V_0-sector of the V-ATPase, synaptobrevin, and synaptophysin are associated on synaptic vesicles in a Triton X-100-resistant, freeze thawing sensitive complex. *J. Biol. Chem.* 271:24534–24537.
26. Garnier, J., D.J. Osguthorpe, and B. Robson. 1978. Analysis of the accuracy and implications of simple methods for predicting the secondary structure of globular proteins. *J. Mol. Biol.* 120:97–120.
27. Gough, N.M. 1988. Rapid and quantitative preparation of cytoplasmic RNA from small numbers of cells. *Anal. Biochem.* 173:93–95.
28. Hansen, S.H., K. Sandvig, and B. van Deurs. 1991. The preendosomal compartment comprises distinct coated and noncoated endocytic vesicle populations. *J. Cell Biol.* 113:731–741.
29. Herrmann, H., I. Hofmann, and W.W. Franke. 1992. Identification of a nonapeptide motif in the vimentin head domain involved in intermediate filament assembly. *J. Mol. Biol.* 223:637–650.
30. Herrmann, H., A. Eckelt, M. Brettel, C. Grund, and W.W. Franke. 1993. Temperature-sensitive intermediate filament assembly. Alternative structures of *Xenopus laevis* vimentin in vitro and in vivo. *J. Mol. Biol.* 234:99–113.
31. Horst, M., N. Harth, and A. Hasilik. 1991. Biosynthesis of glycosylated human lysozyme mutants. *J. Biol. Chem.* 266:13914–13919.
32. Hudson, A.W., and M.J. Birnbaum. 1995. Identification of a nonneuronal isoform of synaptotagmin. *Proc. Natl. Acad. Sci. USA.* 92:5895–5899.
33. Jahn, R., W. Schiebler, C. Ouimet, and P. Greengard. 1985. A 38,000-dalton membrane protein (p38) present in synaptic vesicles. *Proc. Natl. Acad. Sci. USA.* 82:4137–4141.
34. Johnston, P.A., and T.C. Südhof. 1990. The multisubunit structure of synaptophysin. *J. Biol. Chem.* 265:8869–8873.
35. Johnston, P.A., P.L. Cameron, H. Stukenbrok, R. Jahn, P. De Camilli, and T.C. Südhof. 1989. Synaptophysin is targeted to similar microvesicles in CHO and PC12 cells. *EMBO (Eur. Mol. Biol. Organ.) J.* 8:2863–2872.
36. Knaus, P., and H. Betz. 1990. Mapping of a dominant immunogenic region of synaptophysin, a major membrane protein of synaptic vesicles. *FEBS Lett.* 261:358–360.
37. Knaus, P., B. Marquèze-Pouey, H. Scherer, and H. Betz. 1990. Synaptoporin, a novel putative channel protein of synaptic vesicles. *Neuron.* 5: 453–462.
38. Laurie, S.M., C.C. Cain, G.E., Lienhard, and J.D. Castle. 1993. The glucose transporter GluT4 and secretory carrier membrane proteins (SCAMPs) colocalize in rat adipocytes and partially segregate during insulin stimulation. *J. Biol. Chem.* 268:19110–19117.
39. Leimer, U., W.W. Franke, and R.E. Leube. 1996. Synthesis of the mammalian synaptic vesicle protein synaptophysin in insect cells: a model for vesicle biogenesis. *Exp. Cell Res.* 224:88–95.
40. Leube, R.E. 1994. Expression of the synaptophysin gene family is not restricted to neuronal and neuroendocrine differentiation in rat and human. *Differentiation.* 56:163–171.
41. Leube, R.E. 1995. The topogenic fate of the polytopic transmembrane proteins, synaptophysin and connexin, is determined by their membrane-spanning domains. *J. Cell Sci.* 108:883–894.
42. Leube, R.E., P. Kaiser, A. Seiter, R. Zimbelmann, W.W. Franke, H. Rehm, P. Knaus, P. Prior, H. Betz, H. Reinke et al. 1987. Synaptophysin: molecular organization and mRNA expression as determined from cloned cDNA. *EMBO (Eur. Mol. Biol. Organ.) J.* 6:3261–3268.
43. Leube, R.E., B. Wiedenmann, and W.W. Franke. 1989. Topogenesis and sorting of synaptophysin: synthesis of a synaptic vesicle protein from a gene transfected into nonneuroendocrine cells. *Cell.* 59:433–446.
44. Leube, R.E., U. Leimer, C. Grund, W.W. Franke, N. Harth, and B. Wiedenmann. 1994. Sorting of synaptophysin into special vesicles in non-neuroendocrine epithelial cells. *J. Cell Biol.* 127:1589–1601.
45. Li, C., B. Ullrich, J.Z. Zhang, R.G.W. Anderson, N. Brose, and T.C. Südhof. 1995. Ca^{2+}-dependent and -independent activities of neural and non-neural synaptotagmins. *Nature (Lond.).* 375:594–599.
46. Maycox, P.R., E. Link, A. Reetz, S.A. Morris, and R. Jahn. 1992. Clathrin-coated vesicles in nervous tissue are involved primarily in synaptic vesicle recycling. *J. Cell Biol.* 118:1379–1388.
47. McMahon, H.T., Y.A. Ushkaryov, L. Edelmann, E. Link, T. Binz, H. Niemann, R. Jahn, and T.C. Südhof. 1993. Cellubrevin is a ubiquitous tetanus-toxin substrate homologous to a putative synaptic vesicle fusion protein. *Nature (Lond.).* 364:346–349.
48. Messner, D.J., G. Griffiths, and S. Kornfeld. 1989. Isolation and characterization of membranes from bovine liver which are highly enriched in mannose 6-phosphate receptors. *J. Cell Biol.* 108:2149–2162.
49. Nagy, A., J. Rossant, R. Nagy, W. Abramow-Newerly, and J.C. Roder. 1993. Derivation of completely cell culture-derived mice from early-passage embryonic stem cells. *Proc. Natl. Acad. Sci. USA.* 90:8424–8428.
50. Navone, F., R. Jahn, G. Di Gioia, H. Stukenbrok, P. Greengard, and P. De Camilli. 1986. Protein p38: An integral membrane protein specific for small vesicles of neurons and neuroendocrine cells. *J. Cell Biol.* 103:2511–2527.
51. Orci, L., B.S. Glick, and J.E. Rothman. 1986. A new type of coated vesicular carrier that appears not to contain clathrin: its possible role in protein transport within the Golgi stack. *Cell.* 46:171–184.
52. Orci, L., M. Ravazzola, M. Amherdt, A. Perrelet, S.K. Powell, D.L. Quinn, and H.-P.H. Moore. 1987. The *trans*-most cisternae of the Golgi complex: a compartment for sorting of secretory and plasma membrane proteins. *Cell.* 51:1039–1051.
53. Orci, L., V. Malhotra, M. Amherdt, T. Serafini, and J.E. Rothman. 1989. Dissection of a single round of vesicular transport: sequential intermediates for intercisternal movement in the Golgi stack. *Cell.* 56:357–368.
54. Özçelik, T., R.G. Lafreniere, B.T. Archer III, P.A. Johnston, H.F. Willard, U. Francke, and T.C. Südhof. 1990. Synaptophysin: structure of the human gene and assignment to the X chromosome in man and mouse. *Am. J. Hum. Genet.* 47:551–561.
55. Pearse, B.M.F., and M.S. Robinson. 1990. Clathrin, adaptors, and sorting. *Annu. Rev. Cell Biol.* 6:151–171.
56. Pfeffer, S.R., and J.E. Rothman. 1987. Biosynthetic protein transport and sorting by the endoplasmic reticulum and Golgi. *Annu. Rev. Biochem.* 56: 829–852.
57. Pryer, N.K., L.J. Wuestehube, and R. Schekman. 1992. Vesicle-mediated protein sorting. *Annu. Rev. Biochem.* 61:471–516.
58. Ralston, E., S. Beushausen, and T. Ploug. 1994. Expression of the synaptic vesicle proteins VAMPs/synaptobrevins 1 and 2 in non-neuronal tissues. *J. Biol. Chem.* 269:15403–15406.
59. Regazzi, R., C.B. Wollheim, J. Lang, J.-M. Theler, O. Rossetto, C. Montecucco, K. Sadoul, U. Weller, M. Palmer, and B. Thomas. 1995. VAMP-2 and cellubrevin are expressed in pancreatic β-cells and are essential for Ca^{2+}- but not for GTPγS-induced insulin secretion. *EMBO (Eur. Mol. Biol. Organ.) J.* 14:2723–2730.
60. Rossetto, O., L. Gorza, G. Schiavo, N. Schiavo, R.H. Scheller, and C. Montecucco. 1996. Vamp/synaptobrevin isoforms 1 and 2 are widely and differentially expressed in nonneuronal tissues. *J. Cell Biol.* 132:167–179.
61. Rothman, J.E. 1994. Mechanisms of intracellular protein transport. *Nature (Lond.).* 372:55–63.
62. Siebert, A., F. Lottspeich, N. Nelson, and H. Betz. 1994. Purification of the synaptic vesicle-binding protein physophilin. *J. Biol. Chem.* 269:28329–28334.
63. Simons, K., and M. Zerial. 1993. Rab proteins and the road maps for intracellular transport. *Neuron.* 11:789–799.
64. Stenius, K., R. Janz, T.C. Südhof, and R. Jahn. 1995. Structure of synaptogyrin (p29) defines novel synaptic vesicle protein. *J. Cell Biol.* 131:1801–1809.
65. Stoorvogel, W., V. Oorschot, and H.J. Geuze. 1996. A novel class of clathrin-coated vesicles budding from endosomes. *J. Cell Biol.* 132:21–33.
66. Südhof, T.C. 1995. The synaptic vesicle cycle: a cascade of protein-protein interactions. *Nature (Lond.).* 375:645–653.
67. Südhof, T.C., F. Lottspeich, P. Greengard, E. Mehl, and R. Jahn. 1987. A synaptic vesicle protein with a novel cytoplasmic domain and four transmembrane regions. *Science (Wash. DC).* 238:1142–1144.
68. Thomas, L., K. Hartung, D. Langosch, H. Rehm, E. Bamberg, W.W. Franke, and H. Betz. 1988. Identification of synaptophysin as a hexameric channel protein of the synaptic vesicle membrane. *Science (Wash. DC).* 242:1050–1053.
69. Troyanovsky, S.M., R.B. Troyanovsky, L.G. Eshkind, V.A. Krutovskikh, R.E. Leube, and W.W. Franke. 1994. Identification of plakoglobin-binding domain in desmoglein and its role in plaque assembly and intermediate filament anchorage. *J. Cell Biol.* 127:151–160.
70. Ullrich, B., C. Li, J.Z. Zhang, H. McMahon, R.G.W. Anderson, M. Geppert, and T.C. Südhof. 1994. Functional properties of multiple synaptotagmins in brain. *Neuron.* 13:1281–1291.
71. Volchuk, A., Y. Mitsumoto, L. He, Z. Liu, E. Habermann, W. Trimble, and A. Klip. 1994. Expression of vesicle-associated membrane protein 2 (VAMP-2)/synaptobrevin II and cellubrevin in rat skeletal muscle and in a muscle cell line. *Biochem. J.* 304:139–145.
72. Washbourne, P., G. Schiavo, and C. Montecucco. 1995. Vesicle-associated membrane protein-2 (synaptobrevin-2) forms a complex with synaptophysin. *Biochem. J.* 305:721–724.
73. White, S., K. Miller, C. Hopkins, and I.S. Trowbridge. 1992. Monoclonal antibodies against defined epitopes of the human transferrin receptor cytoplasmic tail. *Biochim. Biophys. Acta.* 1136:28–34.
74. Whitney, J.A., M. Gomez, D. Sheff, T. Kreis, and I. Mellman. 1995. Cytoplasmic coat proteins involved in endosome function. *Cell.* 83:703–713.
75. Wiedenmann, B., and W.W. Franke. 1985. Identification and localization of synaptophysin, an integral membrane glycoprotein of M_r 38,000 characteristic of presynaptic vesicles. *Cell.* 41:1017–1028.
76. Wiedenmann, B., W.W. Franke, C. Kuhn, R. Moll, and V.E. Gould. 1986. Synaptophysin: a marker protein for neuroendocrine cells and neoplasms. *Proc. Natl. Acad. Sci. USA.* 83:3500–3504.
77. Zhong, C., D.J. Hayzer, and M.S. Runger. 1992. Molecular cloning of a cDNA encoding a novel protein related to the neuronal vesicle protein synaptophysin. *Biochim. Biophys. Acta.* 1129:235–238.